



Deposited via The University of Leeds.

White Rose Research Online URL for this paper:

<https://eprints.whiterose.ac.uk/id/eprint/203737/>

Version: Accepted Version

Article:

Qiang, W., Jing, G., Connolly, D.P. et al. (2023) The use of recycled rubber in ballasted railway tracks: A review. *Journal of Cleaner Production*, 420. 138339. ISSN: 0959-6526

<https://doi.org/10.1016/j.jclepro.2023.138339>

© 2023, Elsevier. This manuscript version is made available under the CC-BY-NC-ND 4.0 license <http://creativecommons.org/licenses/by-nc-nd/4.0/>.

Reuse

This article is distributed under the terms of the Creative Commons Attribution-NonCommercial-NoDerivs (CC BY-NC-ND) licence. This licence only allows you to download this work and share it with others as long as you credit the authors, but you can't change the article in any way or use it commercially. More information and the full terms of the licence here: <https://creativecommons.org/licenses/>

Takedown

If you consider content in White Rose Research Online to be in breach of UK law, please notify us by emailing eprints@whiterose.ac.uk including the URL of the record and the reason for the withdrawal request.

1 **The use of recycled rubber in ballasted railway tracks: a review**

2 **Weile Qiang ^a, Guoqing Jing ^b, David P. Connolly ^c, Peyman Aela ^d**

3 ^a Railway specialist, Institute of Infrastructure Inspection, China Academy of Railway Science Corporation
4 Limited (CARS), Beijing 100081, China. Email: qiangweile@rails.cn

5 ^b Professor, School of Civil Engineering, Beijing Jiaotong University, Beijing 100044, China. Email:
6 gqjing@bjtu.edu.cn

7 ^c Professor, Institute for High Speed Rail and System Integration, School of Civil Engineering, University
8 of Leeds, Leeds, LS2 9JT, UK, Email: d.connolly@leeds.ac.uk

9 ^d Postdoctoral fellow, Department of Civil and Environmental Engineering, The Hong Kong Polytechnic
10 University, Hung Hom, Kowloon, Hong Kong, China. Email: peyman.aela@polyu.edu.hk

11 **Abstract**

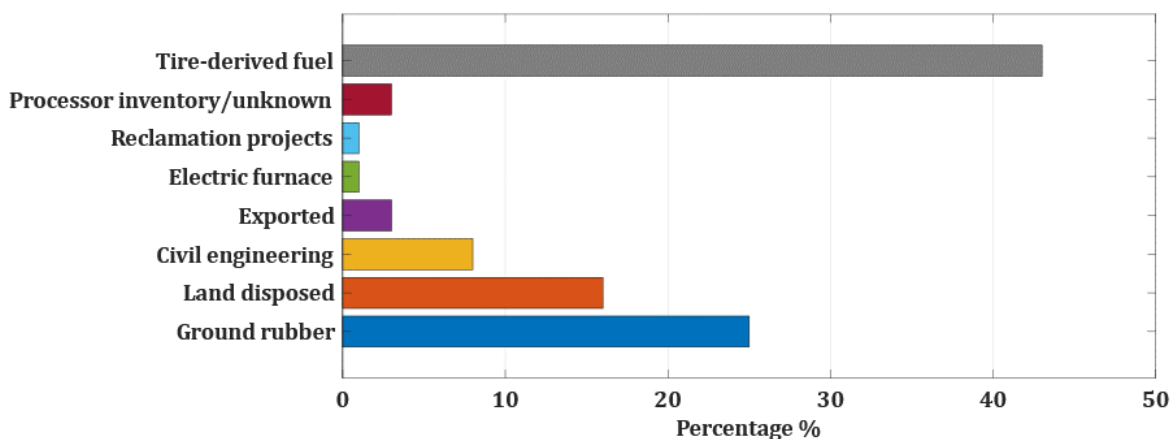
12 The disposal of waste tyre rubber (WTR) is an environmental challenge, and a significant amount of waste
13 is sent to landfills. However, modern railway tracks depend on rubber materials for their resilient elements.
14 Therefore, extensive research is being conducted to investigate the reuse of WTR to form track components.
15 To better understand this body of research, this paper presents a state-of-the-art review of the application
16 of WTR in railways. First, the use of WTR for components close to the rail is explored with a focus on
17 railroads, rail dampers, and level-crossing applications. Next, rubber–concrete sleepers and under-sleeper
18 pads are discussed before exploring ballast-related solutions such as under-ballast mats and ballast mixed
19 with rubber crumbs/chips. Finally, numerical simulation methods are discussed, including finite element
20 constitutive models and the discrete element method. The paper concludes with suggestions for future
21 research.

22 **Keywords:**

23 Waste tire rubber; Ballast rubber crumbs–chips; Under sleeper pads; Railway sustainability;
24 Recycled rubber; Under ballast mat

26 1 Introduction

27 The accumulation and burning of waste tire rubber (WTR) cause severe environmental problems,
28 such as the release of toxic fumes and water and air pollution. Discarded tires can be used as energy
29 sources, such as gasoline, but they should be separated from other rubber products. As shown in
30 Fig. 1, WTR can be used as an alternative fuel in cement kilns and for power generation. However,
31 its combustion pollutes the environment. The standard practice for using WTR in civil engineering
32 is established according to ASTM D6270-20 (2020). In 2017, only 8% of scrap tires were
33 employed in civil engineering-related projects (USTMA, 2019). WTR is a recyclable material, and
34 its recycling and reuse in various geotechnical engineering fields such as landfills, pavements, and
35 embankments have increased considerably (Mohajerani et al., 2020). Because rubber has a
36 relatively low specific gravity (1–1.36) and a suitable damping ratio, it has been extensively used
37 in embankment fills, retaining wall backfills, drainage layers for roads, landfills, thermal insulators,
38 vibration dampers in highway and railway infrastructure, sound barriers, and in mixtures of
39 rubber/soil or rock materials, as reported by Humphrey (2007).



40
41 Fig. 1 Scrap tire disposition in the U.S. modified from (USTMA, 2019)

42 Recently, there has been a tendency to apply WTRs in railway infrastructure as granular mixtures,
43 layered pads, or composite materials to address existing track problems (Fig. 2). Owing to the

44 elastic characteristics of WTRs, the early goal of rubber superstructures was to implement
45 vibration-damping measures in railway embankments. Subsequently, WTRs were used as granular
46 and layered shapes on railway tracks. The long-term performance and cost efficiency of reinforced
47 ballasted tracks are concerns for the further use of WTRs in the railway industry.

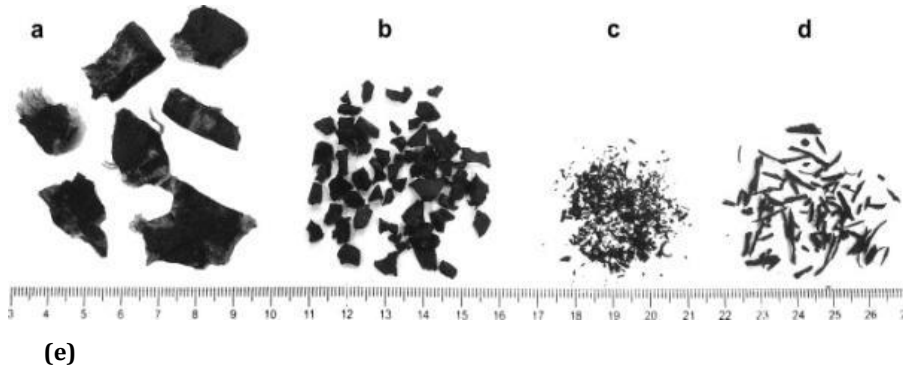


48

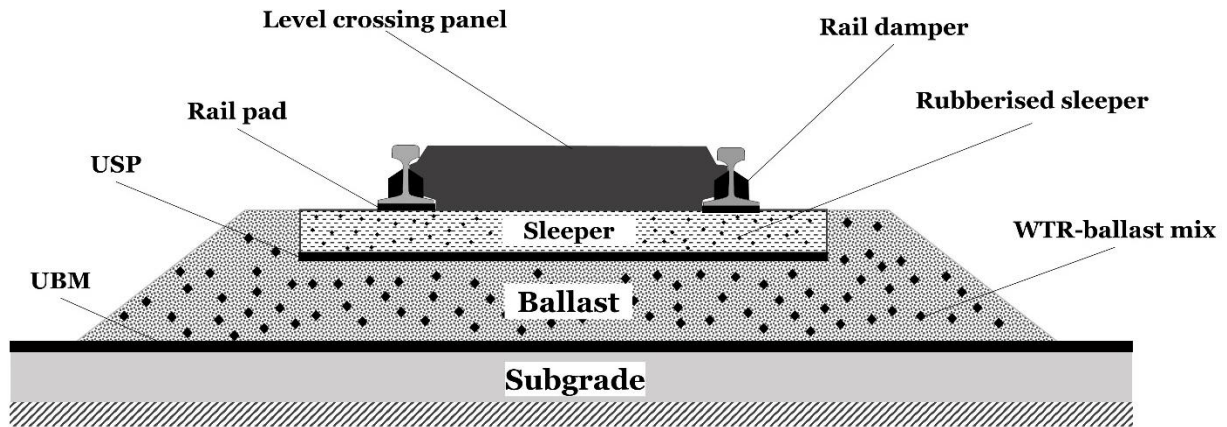
49

50 Fig. 2 The application of WTR: (a) railway embankment (CalRecycle, 2001), (b) under sleeper base (Navaratnarajah
51 et al., 2018), (c) within the ballast layer (Fathali et al., 2019), and (d) under the ballast layer (Kraśkiewicz et al.,
52 2023)

53 The specific gravity and bulk density of WTR range from 0.51 to 1.2 and 524 to 1273 kg/m³,
54 respectively ((Fakhri and Saberi. K, 2016)). Further details on the physical and chemical
55 characteristics of tire rubber can be found in (Siddika et al., 2019). WTRs are used in various forms
56 and sizes in railway superstructures, such as crumbs, powders, and layered pads. The selection of
57 a suitable rubber size and form is vital for producing highly efficient products. Layered WTRs
58 have been used as a rail pad (RP), under sleeper pad (USP), and under ballast mat (UBM), as
59 illustrated in Fig. 3e. From a size perspective, WTRs are categorised into tire shreds (50–305 mm),
60 tire chips (12–50 mm), and crumb rubber (0.425–12 mm), as shown in Fig. 3a-d (ASTM D6270-
61 20, 2020). The CEN Workshop Agreement reported a precise classification of rubber products
62 based on particle size (Table 1).



63
64
65



66
67
68
69

Fig. 3 Rubber aggregates: (a) shredded, (b) crumb, (c) granular, (d) fibre, and (e) rubber layers, modified from (Najim and Hall, 2010)

Table 1 Material Sizes of Tyre Derived Products (TDPs) (Oikonomou and Mavridou, 2009)

| Material | Size |
|----------------|---------------------|
| Cuts | > 300 mm |
| Shred | 50 – 300 mm |
| Chips | 10 – 50 mm |
| Crumb | 1 – 10 mm |
| Powder | < 1 mm |
| Fine powder | < 500 μm |
| Buffings | 0 – 40 mm |
| Pyrolytic char | < 10 mm |

70

71 In addition to rubber size, the percentage of mixed rubber particles is another important parameter
72 that should be considered. The increase in rubber content leads to changes in the mixture behaviour
73 from rigid (plastic) to rubber-like (elastic) owing to the higher probability of contact between the
74 rubber particles.

75 While existing review papers on rubber inclusion in railway infrastructure have mainly focused on
76 the performance of layered WTR at the interface between railway components (Sol-Sánchez,
77 Miguel et al., 2015), recent findings by Mayuranga et al. (2023) explored the use of
78 granular/layered WTR elements in ballasted tracks. Despite this progress, several research gaps
79 must be addressed. Specifically, previous studies have not investigated the application of WTR in
80 the rail zone, which is a primary source of noise and vibration propagation owing to its direct
81 interaction with the train wheels, in components such as rail dampers and level-crossing panels.
82 Additionally, there is a need for a quantitative-based investigation of the effect of WTR-based
83 products on the performance of railway components, as well as guidelines for simulating WTR in
84 railway superstructures, to provide a suitable method for analysing the interaction between WTRs
85 and railway elements. This review aims to address these issues by focusing on three main areas:
86 (I) experimental investigations of the performance of WTR-reinforced track superstructures, (II)
87 numerical methods for simulating rubber-like materials, and (III) potential challenges for future
88 studies using WTR.

89 **2 Use of WTR in ballast track components**

90 Using WTR in ballast track components is an area of active research and development; however,
91 several challenges need to be addressed, including the potential for rubber particles to migrate into
92 the ballast and interfere with the track's structural/dynamic performance. One experimental
93 approach that has been explored is the use of rubber pads placed on the rail seat, at the top or
94 bottom of the ballast layer, which are named under sleeper pad (USP) and under ballast mat
95 (UBM), respectively. The rubber layer may exhibit various mechanical properties depending on

96 the application zone. Because rubber-made layers are widely used in railways, the typical ranges
 97 of properties for different rubber layers are presented in Table 2.

98 Table 2 WTR layer stiffness (Kraśkiewicz et al., 2018) and physical properties (Sol-Sánchez, Miguel et al., 2015)

| Product | Thickness (mm) | Density (kg/m ³) | Stiffness (kN/mm) | C _{stat} (N/mm ³) | C _{dyn} (N/mm ³) |
|---------|----------------|------------------------------|--|---|--|
| RP | 4.5-15 | 950 - 980 | >150 (hard) 80-150 (medium) <80 (soft) | – | – |
| USP | 5.5-20 | 710 - 1100 | ~50 (soft) ~400 (medium) ~3000 (hard) | 0.25–0.45 (hard) 0.15–0.25 (medium) 0.08–0.15 (soft) <0.08 (very soft) | ≥0.25 (hard) 0.09-0.25 (soft) <0.09 (very soft) |
| UBM | 10-52 | 310 - 1000 | – | 0.018 – 0.267 | >0.22 (hard) 0.9-0.22 (medium) 0.05-0.09 (soft) 0.01-0.05 (very soft) |

99 Another approach involves the use of granular WTRs as additives in railway concrete sleepers or
 100 ballast layers. In this case, the performance of the reinforced components is governed by the rubber
 101 size distribution and percentage. Depending on the type and location of the WTR (including rail–
 102 sleeper, sleeper–ballast, and ballast–subgrade interfaces), specific laboratory tests are required to
 103 evaluate the mechanical performance of the WTR-reinforced track. Fig. 4 shows the publications
 104 on WTR inclusion in ballasted railway superstructures. Most studies have focused on rubber
 105 stiffness and its influence on track components.

106 However, little is known about the effects of moisture on the performance of WTR-reinforced
 107 ballast. The following sections describe the experiments conducted on each product. Moreover,
 108 climate change and its impacts have not been well investigated. Regarding rubberised concrete
 109 sleepers, although comprehensive analyses of concrete samples have been carried out, little
 110 research has considered the performance of rubberised concrete sleepers, which requires a specific
 111 mix design and sleeper-related tests.

112

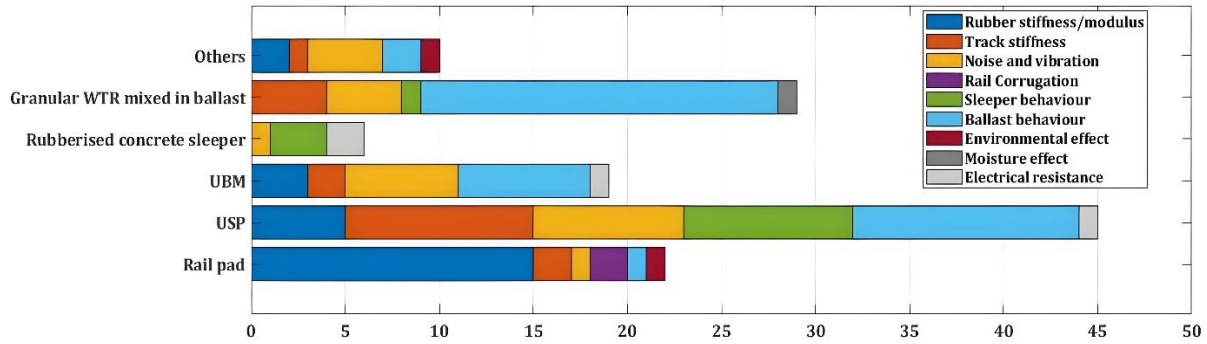


Fig. 4 Previous studies on WTR-reinforced track superstructure

*More studies on rubberised concrete were provided by Mohammed et al. (2017) and Siddika et al. (2019)

2.1 Rail

According to the literature, WTRs can be applied as rubber pads between rails and sleepers or as rail dampers to improve track performance in terms of noise, vibration, and stress transmission characteristics. The stiffness of the layered rubber is an important factor that should be examined when designing efficient elements. Grassie (1989) proposed Eq. (1) to determine the RP stiffness of rail track (k_T) based on the stiffness value obtained from laboratory tests (k_L).

$$k_T = 16.87 + 0.463k_L \quad (1)$$

In the following, the specifications of each type of element are described.

2.1.1 Rail pad

Rail pads (RPs) are typically composed of rubber, high-density polyethylene (HDPE), thermoplastic polyester elastomer (TPE), and ethylene vinyl acetate (EVA). Recycled rubber RPs isolate the rail from the concrete sleepers and reduce noise and vibration. They are typically made from recycled rubber with a thickness of 4.5 to 15 mm and are used in conjunction with springs or elastomeric fastenings to allow for the movement and expansion of the rail (Sol-Sánchez, Miguel et al., 2015). Several factors must be considered when selecting and installing recycled rubber RPs, including the type of rail, track, load, and train speed. The principal characteristic parameter of

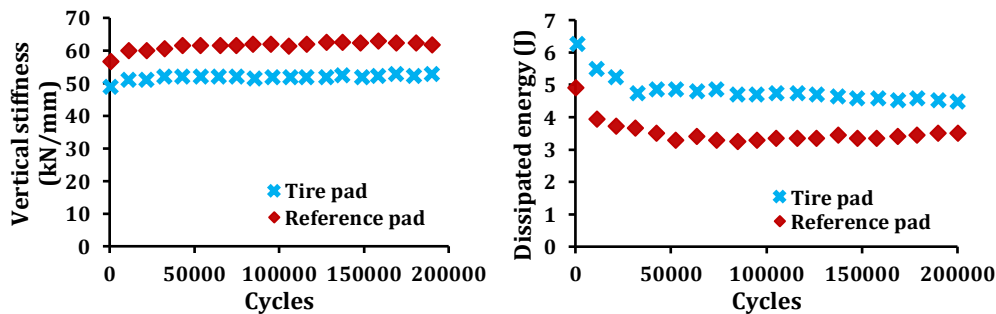
132 RPs is stiffness. British Standard No. 13481-2 and AREMA No. 1-30 provide the test conditions
 133 for measuring the dynamic stiffness of RPs as part of fastening systems. A comparison of these
 134 two standards can be found in (Qi et al., 2022).

135 Studies on the relationship between the stiffness of RPs and the mechanical properties of ballasted
 136 tracks are presented in Table 3. The results show the importance of the RP stiffness in transmitting
 137 stresses into the ballast bed. They also indicate that stiffer RPs are suitable for reducing the rail
 138 vibration and displacement and prolonging the service life of the fastening system, whereas softer
 139 RPs are appropriate for reducing the imposed vertical stress on the ballast and the consequent track
 140 stiffness, sleeper deterioration, rail corrugation, and vibration between the sleeper and ballast bed.

141 Table 3 Laboratory tests on RPs stiffness

| Author | Variable | Findings |
|---------------------------|--|--|
| Giannakos (2010) | Static loading | An increase in pad stiffness from 40 to 250 kN/mm led to a 20% increase in stress on the ballast bed. |
| Teixeira (2004) | Track stiffness | The decrease in RP stiffness below 100 kN/mm reduces the changes in track stiffness. |
| Carrascal Vaquero (2010) | Dynamic loading | Applying repeated loads led to an 18% increase in stiffness and a 40% decrease in dissipated energy. |
| Maes et al. (2006) | Load frequency Preload | A steady trend of dynamic stiffness when the frequency is between 20 and 2000 Hz and a rapid rise of stiffness when the frequency rises up to 2500 Hz |
| Egana et al. (2006) | Rail wave | Reduction in RP stiffness from 90 to 60 kN/mm resulted in a 55% reduction in rail wave. |
| Thompson and Jones (2006) | Noise | Variations when RP stiffness increased from 25 to 8000 kN/mm: Sleeper: +16%; Rail (vertical): -20%; Rail (lateral): -10%; track (total): -11%. |
| Carrascal et al. (2010) | Temperature Severe environmental conditions | 30 % stiffness increment with a 30° C increase in temperature. 33-41% increase in RP stiffness after a life service of 1-3 years. |
| Leykauf and Stahl (2004) | Ballast acceleration | 90% variation of recorded vibration when loading frequency is between 16 and 250 Hz. |
| Ilias (1999) | Rail corrugation | The stiffer pads, the faster the corrugation growth, so an increase in RP stiffness from 280 to 500 kN/mm led to a 72% and 51% increase in wear rate for 100 mm and 300 mm wavelength, respectively. |

142 As shown in Fig. 5, an application of deconstructed tyres as RPs was proposed by Sol-Sánchez et
 143 al. (2014a). A thickness of 7.5–9 mm was proposed as the most efficient tire RPs under static and
 144 dynamic loading conditions. The research findings indicated that using a tire pad in the system
 145 caused a slight reduction in vertical stiffness, likely because of its lower dynamic stiffness
 146 compared to that of a rubber pad. The dynamic test results showed that the tire pad had a vertical
 147 stiffness of approximately 52.5 kN/mm, which is similar to that of the commercial pad
 148 (approximately 61.5 kN/mm). This suggests that tire pads could be a viable replacement for
 149 traditional RPs. Moreover, the dissipated energy levels for both types were fairly similar (mean
 150 value near 4.94 J for tire pads and 4.75 J for commercial pads).

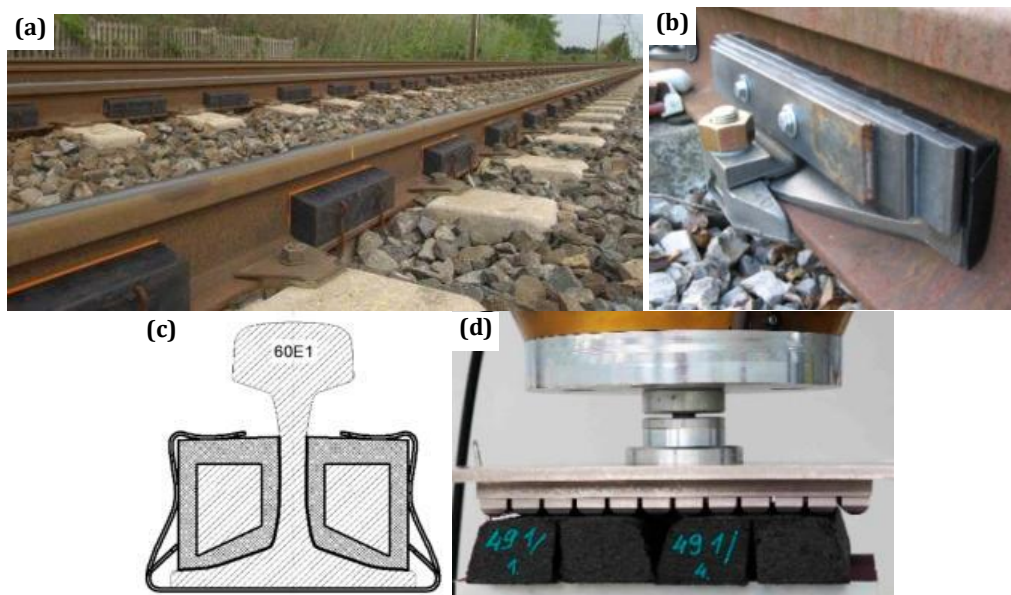


152 Fig. 5 Ballast box test on deconstructed tire-made RPs (Sol-Sánchez et al., 2014b)
 153

154 **2.1.2 Rail damper**

155 Rubber-made rail dampers are another railway application for WTRs (Fig. 6). Rail dampers are
 156 manufactured using either rubber or rubber–steel plate assemblies. Rail dampers are passive
 157 components attached to either side of a rail web to decrease rail noise and vibration. Given the

158 results of compression and tension under severe freezing conditions, Kraškiewicz et al. (2021)
159 stated that the density of manufactured rail dampers should be greater than 1000 kg/m^3 ,
160 corresponding to a static bedding modulus of 0.426 N/mm^3 when the range of the applied stress is
161 $0.02\text{--}0.07 \text{ N/mm}^2$. In addition, dynamic tests showed the frequency dependence of the rail damper
162 on the performance; therefore, an increase in the loading frequency from 1 to 20 Hz led to an
163 increase in the dynamic bedding modulus from 0.219 to 0.448 N/mm^3 .



164

165

166 Fig. 6 (a) Rail damper in a ballasted track (Zvolenský et al., 2017), (b) rubber-steel plate damper (Toward and
167 Thompson, 2012) (c) Cross-section of dynamic rail damper with a steel insert and a rubber cover, (d) compression
168 test on representative ballast plate and rail damper (Kraškiewicz et al., 2021)

169 2.1.3 Rubber level crossing panel

170 WTRs can be used as materials for level crossings in railway systems (Fig. 7). Rubber provides a
171 durable and flexible surface that can withstand heavy axle loads and constant train movements.
172 The advantages of using WTR at railway-level crossings include noise reduction, improved track
173 safety and durability, reduced track maintenance costs, and the prevention of rail deterioration
174 owing to snow residue and road salt. Further, (Hans Bendtsen, 2007) reported a 1-2 dB noise level
175 reduction when using rubber level crossings.



176
177

Fig. 7 Installation of rubber level crossing (a) in the UK (RosehillRail, 2022), (b) in Germany (STRAIL, 2022)

178 2.2 Sleeper

179 Railway sleepers are superstructural components that transmit loads from the rail to the ballast
180 bed. They can be formed from various materials such as concrete, timber, steel, and composites.

181 WTRs can be used either as a powder/crumb mixed with concrete or as a pad underneath the
182 sleeper base (USP). In the first group, concrete-related tests were performed to evaluate the
183 applicability of rubberised concrete samples, whereas the performance of rubber pads was assessed
184 according to the standards for elastomers and railway sleepers, in which rubber stiffness is the
185 primary concern.

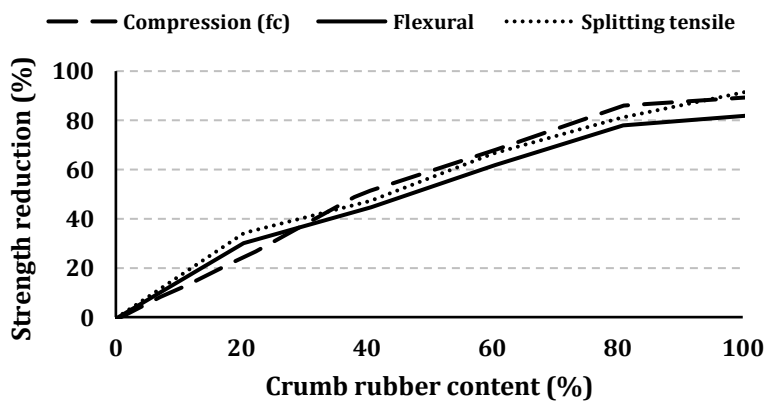
186 2.2.1 Powder/crumb rubber concrete

187 Railway sleepers are superstructural components that transmit loads from the rail to the ballast
188 bed. They can be formed from various materials such as concrete, timber, steel, and composites.

189 WTRs can be used either as a powder/crumb mixed with concrete or as a pad underneath the
190 sleeper base (USP). In the first group, concrete-related tests were performed to evaluate the
191 applicability of rubberised concrete samples, whereas the performance of rubber pads was assessed
192 according to the standards for elastomers and railway sleepers, in which rubber stiffness is the

193 primary concern (Li et al., 2014). Powder and crumb rubber can be used as a replacement for fine
 194 aggregates in concrete sleeper construction. Previous studies have highlighted the importance of
 195 rubber size on concrete behaviour; however, the nanoscale mixture of rubber concrete samples has
 196 not yet been assessed (Mohammed et al., 2017). Kaewunruen et al. (2018) stated that finer crumb
 197 rubber sizes decrease the damping and increase the compressive strength of concrete by filling the
 198 spaces in the concrete. However, replacing fine aggregates with microscale crumb rubber can
 199 enhance the electrical resistance of concrete.

200 Table 4 presents the laboratory tests performed on the RC samples. Generally, the compressive,
 201 tensile, and flexural strengths and elastic modulus decrease after adding WTR to concrete samples
 202 (Fig. 8), whereas higher impact and fatigue resistances are achieved compared with conventional
 203 concrete sleepers. In addition to its mechanical properties, rubberised concrete is vulnerable to
 204 changes in temperature; therefore, adding more rubber reduces the resistance of concrete (Siddika
 205 et al., 2019).



206 Fig. 8 The effect of rubber content on concrete strength parameters (Batayneh et al., 2008)

207 Table 4 Changes in the mechanical behaviour of rubberised sleepers compared to the conventional type

| Author | Rubber size and content | Measured parameters | Findings |
|--------|-------------------------|---------------------|----------|
|--------|-------------------------|---------------------|----------|

| | | | |
|------------------------------|--|---|---|
| Hameed and Shashikala (2016) | d_{\max} : 12.5 mm RC _v : 15% | Impact resistance Fatigue strength | 80-110% increase in resistance to crack initiation 40-60% increase in impact strength |
| Siahkouhi et al. (2022) | d: 0.28 mm RC _v : 5, 10, 15% | Compressive, flexural and tensile strength | 28-34% reduction of compressive strength 6-10% reduction of flexural strength About 10% reduction in tensile strength |
| Jing et al. (2022) | d: 0.28 mm RC _v : | Load for Crack initiation Load for crack branching | 20% higher load for crack initiation 20 kN lower load for crack branching |
| Meesit and Kaewunruen (2017) | d: 425, 75 μ m RC _w : 5, 10% | Damping ratio | 42% increase in damping ratio for 425 μ m rubberised concrete samples |
| Noaman et al. (2016) | d: 1.18-2.36 mm RC _v : 5 – 15% | Compressive strength Elastic modulus | 12.7-26% reduction in compressive strength 9.4-18.5% reduction of elastic modulus |
| Akinyele et al. (2015) | RC _v : 4 – 16% | Tensile strength Crack initiation Chemical properties | 41% and 58% decrease in tensile strength when 4% and 16% rubber were added, respectively Reduction in the bond between cement paste and aggregates in the presence of water |
| Bompa et al. (2017) | d: 0 – 20 mm RC _v : 0, 5, 10, 15, 20% | Uniaxial compression strength Modulus of elasticity | Compression $f_{cr} = \frac{1}{1+2\left(\frac{3\lambda\rho_{vr}}{2}\right)^{3/2}} f_{c_0}$ Elastic modulus $E_{cr} = 12 \left(\frac{f_{cr}}{10}\right)^{2/3}$ Tensile strength $f_{ctr,sp} = 0.24 f_{cr}^{2/3}$ |
| Feng et al. (2022) | d: 1-3; 3-5 mm RC _v : 5, 10, 15, 20, 30% | Compressive strength Bonding splitting tensile strength Rubber size | The decrease of the bond splitting tensile strength for rubberised concrete. 10% RC reaches the maximum tensile strength. Compressive and tensile strengths of 3-5 mm-made rubber concrete are greater than that of mixed with 1–3 mm rubber. |

209 λ : A function of the replaced mineral aggregate size ($2 < \lambda < 3$); ρ_{vr} : Volumetric replacement factors
210 In addition to testing the rubber concrete mixture, the mechanical behaviour of the rubber concrete
211 sleeper should be considered. As stated by Zeng et al. (2020), the application of rubberised sleepers
212 can result in vibration reduction in the ballast (2.32 dB) and ground (1.69 dB). Jing et al. (2022)
213 reported the initiation of crack propagation at a lower vertical force for rubberised concrete
214 sleepers compared to conventional ones, which could be associated with the nonuniform mixture
215 of rubber cement or the size of the crumb rubber (Fig. 9).

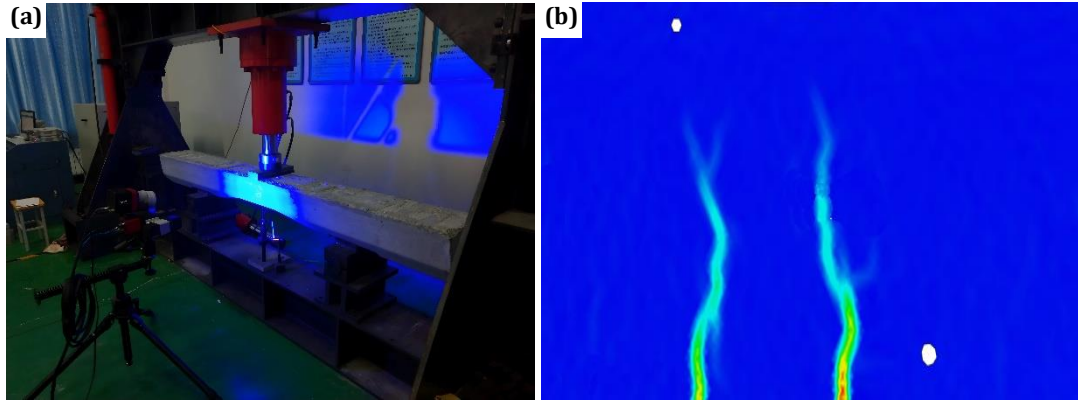


Fig. 9 (a) Measurement of crack propagation on rubberised concrete using DIC, (b) crack growth throughout the sleeper height (Jing et al., 2022)

216
217
218

219 Given some of the challenges associated with rubberised concrete sleepers, manufacturing
220 concrete sleepers with an outer shell made of WTR is an alternative approach for maintaining the
221 structural performance of the sleeper while providing environmental advantages in terms of
222 railway maintenance and sleeper replacement (Dolci et al., 2020).

223 Ferdous et al. (2021) investigated the performance of waste rubber concrete-filled FRP tubes with
224 external flanges as railway sleepers and indicated the low efficiency of rubber concrete in a tube
225 structure (Fig. 10). Owing to the lower strength (9 MPa) and elastic modulus (17 GPa) of
226 rubberised concrete compared with those of ordinary Portland cement (OPC) concrete (30 MPa
227 strength and 25 GPa elastic modulus) as infill material, adding 25% crumb rubber to OPC concrete
228 reduced the moment capacity by 17%, bending stiffness by 1%, horizontal plane shear by 9%, and
229 vertical plane shear by 10%. However, the specimen filled with rubberised concrete was 9% lighter
230 and more durable than that filled with normal concrete.

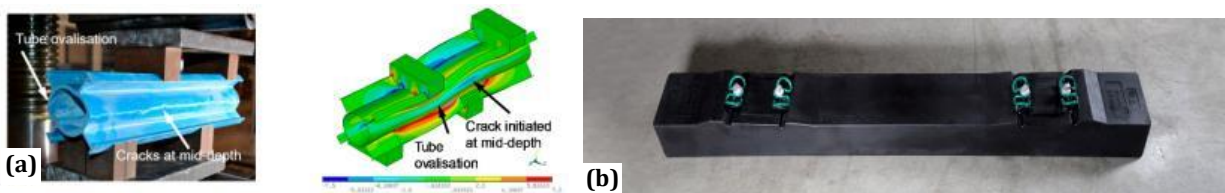
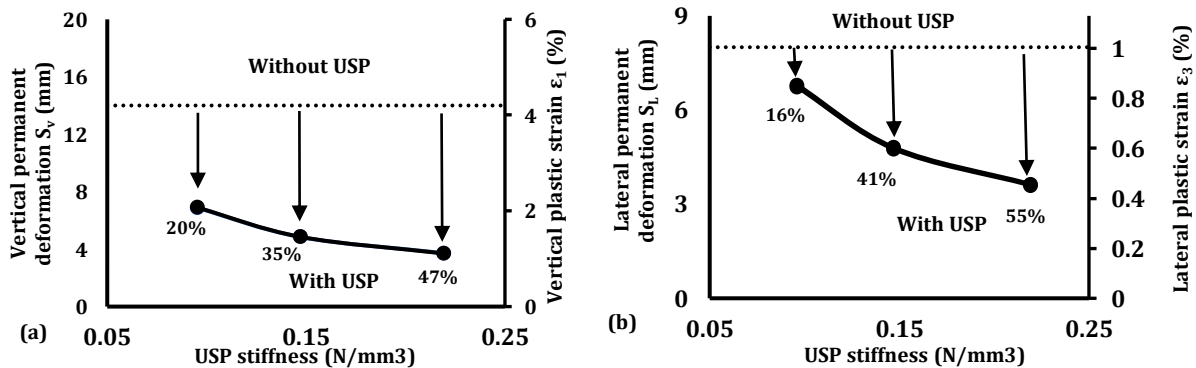


Fig. 10 (a) Experiments and numerical analysis of FRP tube performance (Ferdous et al., 2021), (b) Concrete sleeper covered with a shell of WTR (Jing et al., 2021)

231
232
233

234 **2.2.2 Under Sleeper Pad (USP)**

235 The use of WTR as a USP is effective in reducing vibrations, ballast degradation (Johansson et al.,
 236 2008), and delaying rail corrugation (Mayuranga et al., 2020). BS_EN16730 (2016) outlines
 237 mandatory and optional tests for the mechanical behaviour of USPs, which include static and low-
 238 frequency dynamic bedding modulus tests and fatigue tests. The medium stiff USP ($0.15 < C_{stat} \leq$
 239 0.25) has been identified as an appropriate type for different locations (Ngamkhanong and
 240 Kaewunruen, 2020). Previous studies evaluated the performance of USPs in terms of vibration,
 241 track settlement, lateral track resistance, and stress distribution at the sleeper/ballast interface
 242 (Table 5). The results show that USPs increase the sleeper/ballast contact area and reduce the
 243 ballast vibration and degradation caused by trains. Hard USPs positively increase the ballast lateral
 244 and vertical resistance and reduce rail corrugation (Fig. 11), whereas soft USPs are beneficial for
 245 improving the ballast layer performance .



246 Fig. 11 (a) Vertical and (b) lateral deformation of the ballast sample at the end of the cyclic loading test with and
 247 without USP (Indraratna et al., 2021)
 248

249 Table 5 Studies on ballast performance using USP-reinforced sleepers

| Author | Test type (Standard) | Parameters | Findings |
|------------------------------|----------------------|---|---|
| Navaratnarajah et al. (2018) | Ballast box test | USP depth: 10 mm Subballast dry density: 2115 kg/m ³ Subballast moisture: 10% Load frequency: 15, 20 Hz | 19-29% decrease in ballast settlement 9-14% decrease in ballast lateral displacement |

| | | | | |
|-----------------------------|----------------------------|--|---|--|
| | | | Load amplitude: 250, 350 kN Load cycles: 5e+05 | 37-43% and 53-60% increase in ballast vertical and lateral displacement when axle load increase from 250 to 350 kN 51-57% and 27-33% increase in vertical and lateral displacement when loading frequency increased from 15 to 20 Hz. 50% reduction in ballast breakage |
| Jing et al. (2018) | STPT (UIC) | | USP depth: 10 mm USP bump height: 6, 10 mm Ballast depth: 350 mm | 25% increase in the lateral resistance of steel sleepers |
| Esmaeili et al. (2022) | Cyclic box test (ASTM-CEN) | | Ballast depth: 450 mm USP depth: 12, 13 mm USP modulus: 0.13, 0.3 N/mm ³ Load frequency: 3 Hz Load amplitude: 43 kN | 16.6 % reduction in ballast settlement 7.9 % reduction in ballast breakage 34.6 % reduction in ballast stiffness 114.6 % increase in ballast damping |
| Müller and Brechbühl (2013) | Field test (CEN) | | C _{stat} : 0.11-0.13 N/mm ³ C _{dyn} : 0.14-0.16 N/mm ³ | 33% reduction in ballast settlement using soft USP. 40% reduction in lateral track resistance. |
| Sol-Sánchez et al. (2017) | Ballast box test | | The USP-like layer of stone rubber blowing under the sleeper Rubber size: 8 – 25 mm Rubber thickness: 2.5 mm (hard), 4.5 mm (soft) RC _v : 10, 25, 50% | Injecting 50% rubber particles over a layer of small stones is recommended, resulting: 14-20 mm is recommended rubber size 91% reduction in ballast settlement compared to pure stoneblowing 50% reduction in ballast stiffness 90% reduction in ballast breakage (BBI) 33% higher density of dissipated energy 34% reduction of pressure on subgrade 1500-2000 cm ³ WTR is recommended value for lateral resistance increment |
| Guo et al. (2020b) | Ballast box test | | USP depth: 6 mm USP bedding modulus: 0.212 N/mm ³ Ballast bulk density: 2050 kg/m ³ Load amplitude: 125 kN Load frequency: 8 Hz | 35% reduction in ballast settlement 4-5% reduction in ballast breakage 13.3% increase in ballast-sleeper contact |
| Omodaka et al. (2017) | Single-tie push test | | USP stiffness: 6.5, 8 kN/mm | 18-20% increase in lateral resistance 20-40% reduction in ballast settlement |

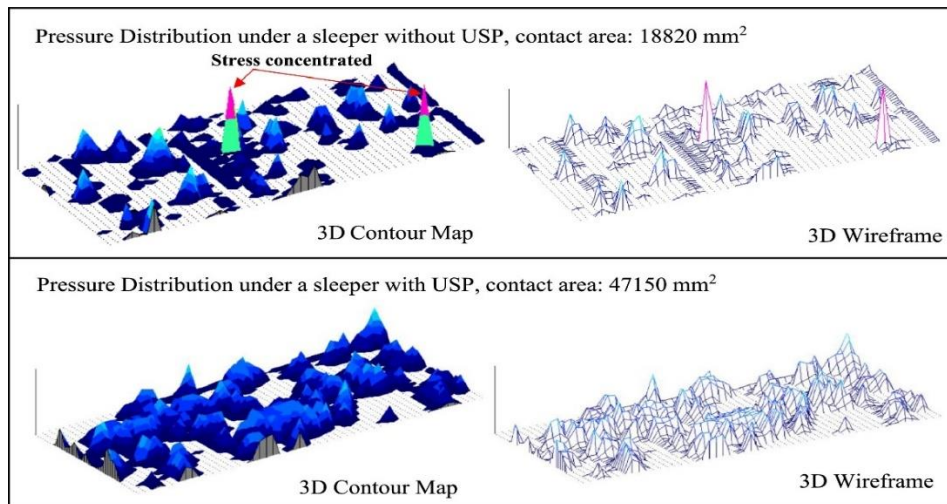
250 ASTM: American Society for Testing and Materials; CEN: European Committee for Standardization;

251 UIC: International Union of Railways

252 More recently, contradictory findings have been reported regarding the vibration characteristics of
253 track components with and without USPs. According to tests conducted by Loy (2008) and
254 Indraratna et al. (2021), the rate of sleeper–ballast contact increased by up to 30%–35% for

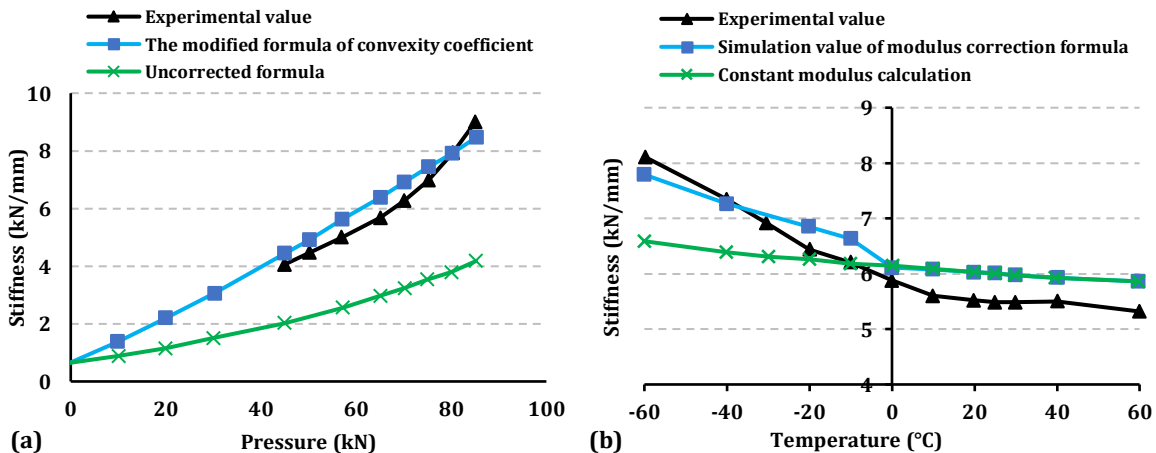
255 sleepers reinforced with USP (Fig. 12), resulting in a 10%–25% reduction in ballast stresses and a
 256 40%–60% reduction in ballast breakage, as reported by Mayuranga et al. (2020). From a vibration
 257 perspective, using USPs leads to lower vibration velocities than conventional sleepers for
 258 frequencies greater than 16 Hz (Stahl, 2005). Field test findings by Marschnig et al. (2022) indicate
 259 that USPs operate better on 20 cm ballast beds than normal concrete sleepers, which makes USPs
 260 appropriate solutions when external boundary constraints, such as those in bridges or tunnels,
 261 require a low ballast depth. By contrast, Schneider et al. (2011) stated that using USPs with $C_{stat} =$
 262 0.3 N/mm^3 led to a 2-3 times increase in sleeper vibration, although the displacement decreased
 263 by 10-15%. Therefore, the USP stiffness and track conditions are essential parameters influencing
 264 the track vibration behaviour, causing different impacts of USPs on ballasted tracks.

265 The static and dynamic stiffnesses of USPs are in the range of $0.12\text{--}0.19 \text{ N/mm}^3$ and $0.17\text{--}0.23$
 266 N/mm^3 , respectively (PANDROL, 2021). Stiffer pads are advantageous when the field
 267 requirement for USPs is to reduce the rail and sleeper vibrations, sleeper acceleration, rail
 268 deflections, rail-bending moments, and corrugation. Alternatively, soft USPs are useful for
 269 minimising settlement and ballast vibration, as recommended by Mayuranga et al. (2020).



270
 271 Fig. 12 Stress distribution under a sleeper with and without USP under cyclic loading (Indraratna et al., 2021)

272 Temperature also affects rubber behaviour, and a 3.5 MPa decrease in Young's modulus was found
 273 when the temperature rose from -60° to 0° . The corresponding formulation for calculating the
 274 nonlinear stiffness of rubber pads at different temperatures and pressures can be found in (Xu et
 275 al., 2020). Fig. 13a-b depict the effect of pressure and temperature on the rubber stiffness at a
 276 temperature of 25°C and a pressure of 57 kN , respectively. The graphs indicate that the rubber
 277 stiffness decreased as the temperature increased, whereas it increased at higher pressures. The
 278 stiffness increased by 38% when the temperature dropped from 0 to -60°C . However, the impact
 279 of temperature on the stiffness was less significant when the temperature was above 0°C .
 280 Conversely, maintaining a constant temperature while increasing the pressure from 45 to 85 kN
 281 resulted in a 100% increase in USP stiffness. The findings from these experiments suggest that
 282 both temperature and pressure have a significant impact on the stiffness of rubber materials such
 283 as USP. Temperature has a more pronounced effect on stiffness at lower temperatures. These
 284 results highlight the importance of considering both temperature and pressure in the design and
 285 performance evaluation of USPs.

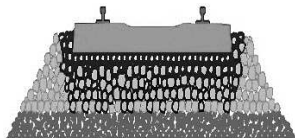




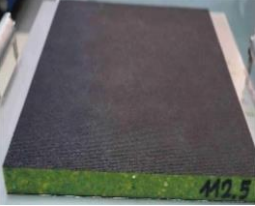

286 Fig. 13 Relationship between (a) temperature, (b) pressure and stiffness of rubber pads (Xu et al., 2020)
 287

288 **2.3 Ballast**

289 Granular WTR is a typical type of WTR used as a mixture with ballast (Sol-Sánchez, M. et al.,
 290 2015), whereas layered WTR (Ballast Mat (BM)) is placed beneath the ballast layer. Different
 291 parameters are measured depending on the type of WTR used within or beneath the ballast layer,
 292 as described in the following subsections. As presented in Table 6, several methods have been
 293 proposed for the application of WTRs to ballast layers, including resiliently bound ballast, rubber-
 294 coated ballast, dry granular WTR–ballast mixtures, ballast mats, and tire-infilled granular waste
 295 materials (Indraratna et al., 2022b). The use of granular and layered WTR is a common approach
 296 for rubber inclusions in railway superstructures. Generally, the proposed methods significantly
 297 reduce ballast layer vibration and particle degradation; however, the construction cost and impact
 298 on ballast layer stiffness differ depending on the preparation process and additive materials (e.g.,
 299 resin and epoxy binder).

300 Table 6 Granular WTR reinforced ballast layer methods

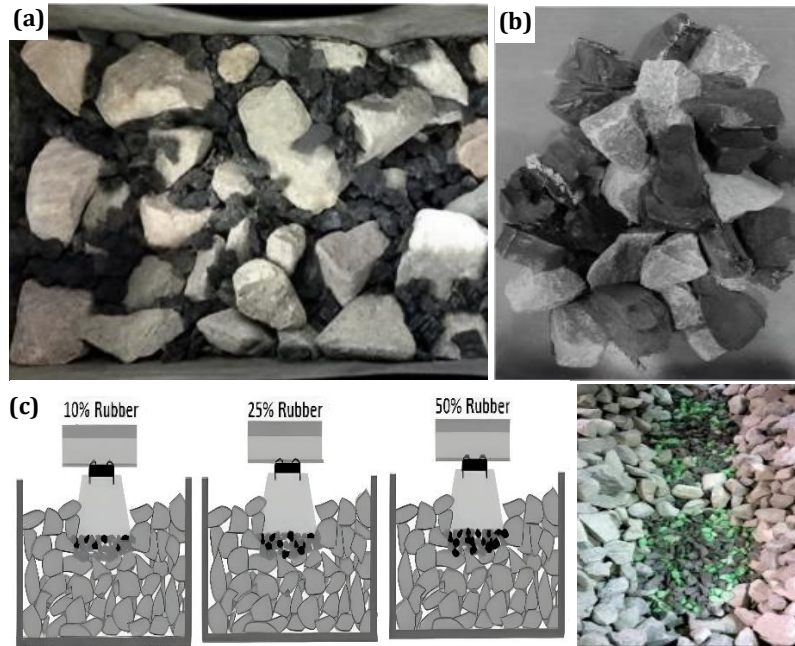
| Ballast-granular WTR- types | Description | Pros and Cons | View |
|--|--|--|---|
| Resiliently Bound Ballast (Ho et al., 2013) | A stable mixture of ballast and WTR bound together with a resilient epoxy binder | <ul style="list-style-type: none"> • Increase in sleeper/ ballast interaction • High vertical stiffness • Less ballast breakage but higher ballast abrasion |  |
| Rubber-Coated Ballast Esmaeili and Namaei (2022); Fontserè et al. (2016) | Coating ballast with powder or crumb rubber using binder/resin | <ul style="list-style-type: none"> • Less maintenance • Less ballast height • Higher construction cost • Less ballast breakage • The stiffness independency upon the mother rock type |  |

| | | | |
|--|--|---|---|
| <p>Dry granular WTR-Ballast mixture (Sol-Sánchez, M. et al., 2015)</p> | <p>The volumetric or gravimetric mixture of granular WTR and ballast</p> | <ul style="list-style-type: none"> • Less construction cost • Difficulties on uniform distribution of WTR within the ballast layer • Directly exposed to the solar thermal effects • Filling ballast gaps and disturbance of ballast drainage |  |
| <p>UBM (Kraśkiewicz et al., 2022)</p> | <p>Placement of a rubber pad under the ballast layer</p> | <ul style="list-style-type: none"> • Easy installation • Reduction of imposed stress on subgrade • Ballast fouling prevention from subgrade • Higher construction cost |  |
| <p>Tire-infilled granular waste materials (Indraratna et al., 2022a)</p> | <p>Placement of rubber tire-confined capping layer as a subballast layer</p> | <ul style="list-style-type: none"> • Less maintenance • Higher lateral resistance • 40% reduction of vertical stress on subgrade |  |

301 **2.3.1 Ballast mixed with granular WTRs**

302 Researchers have investigated the suitability of dry granular WTR mixed with ballast for railway
303 tracks. The optimum size and percentage of granular WTR have been studied in terms of
304 settlement, degradation, and energy dissipation (Table 7). Crumb rubber and rubber chips (ballast
305 size WTR) are the most common mixing sizes Fig. 14a-b. Arachchige et al. (2022b) proposed an
306 optimum size for granular WTR, 9.5 to 19 mm, to reduce ballast degradation. Using WTR in the
307 ballast layer leads to a decrease in ballast stiffness, vibration, and degradation, and an increase in
308 ballast damping. However, a reduction in ballast stiffness may cause dynamic-related problems
309 due to passing trains. The volumetric percentage of the mixed rubber content should be less than
310 10%; however, an appropriate rubber content should be selected based on the track specifications.
311 Moisture content and temperature variations have not been studied extensively and should be
312 considered in future studies. Additionally, Sol-Sánchez et al. (2017) proposed the innovative idea
313 of stone-rubber blowing under a sleeper to improve lateral stability and act as a USP. The results

314 indicated that an amount of 1500-2000 cm³ of WTR could reduce the ballast stiffness, settlement,
 315 and breakage while improving the lateral stability (Fig. 14c).



316

317
 318
 319
 320
 321

Fig. 14 (a) Crumb rubber-ballast (Sol-Sánchez, M. et al., 2015) and (b) chips rubber-ballast samples (Fathali et al., 2017), (c) WTR-stone blowing under the sleeper (Sol-Sánchez et al., 2020)

Table 7 Studies on applied granular WTR into the ballast layer

| Author | Test type | Characteristics | Findings |
|----------------------------------|--|--|---|
| Guo et al. (2019) | Los Angeles abrasion test and Image analysis | Rubber size: 3 – 25 mm RC_w : 0, 10, 20, 30% Surface texture index: $STI = (A_1 - A_2)/A_1$ | <ul style="list-style-type: none"> • Insignificant reduction of ballast degradation using ballast-size WTRs • Less impact on ballast breakage but a considerable effect on ballast abrasion reduction • 10% is optimum RC mixed with ballast |
| Arachchige et al. (2022a, 2022b) | Triaxial compression test | Rubber size: 9.5 – 37.5 mm RC_w : 0, 5, 10, 15% Confining pressures: 10-60 kPa Modulus degradation: E/E_i | <ul style="list-style-type: none"> • 9.5–19 mm is recommended rubber size to preserve ballast strength and reduce ballast breakage • Reduction of modulus degradation up to 10% RC_w • 6% decrease in friction angle for 15% RC_w sample • 50% reduction in the dilation angle when $RC_w > 10\%$ • 15% increase in strain energy density when $RC_w = 10\%$ • 30 and 80% reduction in ballast breakage when RC_w is 10 and 15%, respectively |
| Sol-Sánchez et al. (2017) | Ballast box test | A USP-like layer of stone-rubber blowing under the sleeper Rubber size: 8 – 25 mm Rubber thickness: 2.5 mm (hard), 4.5 mm (soft) RC_v : 10, 25, 50% | Stone + 50% Rubber blowing is recommended mixture, resulting in the following: <ul style="list-style-type: none"> • 91% reduction in ballast settlement compared to pure stoneblowing • 50% reduction in ballast stiffness • 90% reduction in ballast breakage (BBI) • 33% higher density of dissipated energy |

| | | | |
|--|--|---|---|
| | | | <ul style="list-style-type: none"> • 34% reduction of pressure on subgrade • 1500-2000 cm³ is the optimum amount of WTR for improving resistance |
| Esmaeili et al. (2017) | Ballast box test | Adding ballast-size WTRs RC _w : 5, 10, 15% | <ul style="list-style-type: none"> • 5% RC_w is recommended Ballast-WTR mixture • 15% reduction in ballast breakage for 5% RC_w (B_g index) • 28% increase in ballast damping ratio for 10% RC_w • 33% reduction in ballast stiffness • Ballast moisture content should be lower than 5% for the efficient act of WTR • Ballast-WTR settlement formula: $S = 0.007 \times T^2 \times (F + 20)^{0.153} \times Ln N$ |
| Koohmishi and Azarhoosh (2020, 2021, 2022) | Permeability test Impact loading test | Rubber size: 2 – 25 mm RC _v : 10, 20, 30 % Ballast gradations: AREMA_No. 3, 4, and 25 | <p>Reported results for AREMA No. 4:</p> <ul style="list-style-type: none"> • Averagely 36% reduction of ballast hydraulic conductivity when RC increased from 10 to 30% • 18, 28, and 42% increase in hydraulic conductivity when rubber size increased from 2-4.75 mm to 12.5-25 mm, and RC is 10, 20, and 30%, respectively • Higher resistance against impact loads using rubber size of 4.75-9.5 mm • 10% RC_v is recommended regarding vertical deformation |
| Zhang et al. (2022) | Impact loading test | Rubber size: 8 – 16 mm RC _v : 0, 5, 10, 15% | <ul style="list-style-type: none"> • The effect of WTR on ballast breakage is independent of particle morphology • Increase of ballast degradation when RC raised from 0 to 5% • The greatest rubber impact on ballast with the size of 25 – 35.5 mm |
| Song et al. (2019) | Direct shear test | Rubber size: 10 – 50 mm RC _v : 0, 5, 10% Ballast gradation: AREMA 4A Normal stress: 30, 50, 70 MPa N: 300 cycles | <ul style="list-style-type: none"> • 5% is proposed as the optimum RC mixed with ballast • 15% increase in ballast damping ratio • 10% reduction in resilient shear stiffness and friction angle |

322 ϵ_a : Axial strain; E_i : Initial tangent modulus; $E = \Delta q / \Delta \epsilon_a$; S: Settlement;
323 N: Number of load cycles; T: Rubber content; F: Fouling percentage

324 2.3.2 Under Ballast Mat (UBM)

325 WTR can be employed in the form of pads under a ballast layer, which is known as a ballast mat
326 (Fig. 2d). UBMs are typically composed of two layers of polymeric material: (I) a distribution
327 layer to evenly distribute loads and (II) an elastic layer to attenuate stresses. To reduce costs,
328 alternative composites made from recycled tires are being explored in addition to traditional elastic

329 materials. Similar to the testing of a single USP, BS_EN17282 (2020) proposed specifications for
330 UBMs in which fatigue testing is mandatory. Kraśkiewicz et al. (2022) conducted comprehensive
331 experimental tests on the performance of UBMs composed of diverse materials under severe
332 environmental conditions or subjected to cyclic loading conditions. They found that exposure to
333 water, frost, and cyclical loads can permanently alter the static and dynamic properties of elastic
334 elements in railway superstructures. This can potentially affect the effectiveness of vibration
335 reduction throughout the lifespan of railway tracks.

336 UBMs are primarily used to decrease vibrations transmitted to subgrades. Research results in
337 Germany indicated a 15 dB reduction (~30%) for frequencies higher than 31.5 Hz compared with
338 a conventional track (Werkstoffe, 2006). The application of the UBM is promising in cases where
339 stress reduction on the substructure is a concern (e.g., in tunnels, bridges, and switches). In this
340 regard, the thickness and density of the mat and the size and type of the constitutive material are
341 influential parameters. Sol-Sánchez, Miguel et al. (2015) found that soft UBMs can be beneficial
342 as they decrease ballast pressure, degradation, and ground vibration and increase track damping.
343 The utilisation of circular and square aperture GRIDMAT was respectively suggested in recent
344 publications by Sol-Sánchez et al. (2022) and Siddiqui et al. (2023), who merged the properties of
345 the geogrid and ballast mat to simultaneously enhance both track stability and damping (Fig. 15).
346 To achieve optimal efficiency, a highly efficient GRIDMAT with an aperture size of 50–60 mm
347 and a void area of up to 25% was recommended. The study demonstrated that this type of
348 GRIDMAT resulted in a 10% decrease in ballast settlement compared with the UBM-reinforced
349 ballast layer.

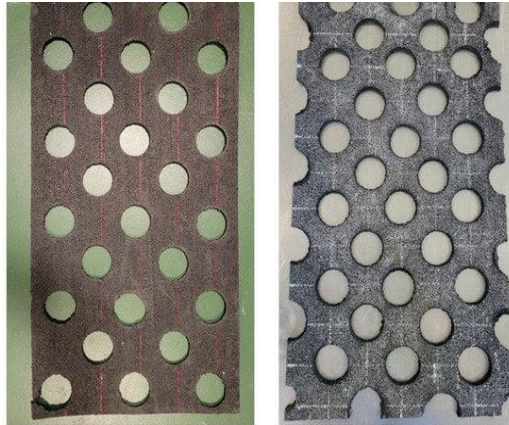


Fig. 15 Different shapes of rubber grid mats used as UBM (Sol-Sánchez et al., 2022)

350
351

352 According to previous studies, the mechanical behaviour of UBM-reinforced ballast has been
353 investigated in terms of ballast settlement, stress distribution, ballast breakage, track noise, and
354 vibration, as presented in Table 8.

355

Table 8 Studies on the performance of the UBM-reinforced ballast layer

| Author | Test type | Characteristics | Findings |
|--------------------------------------|---------------------|---|---|
| Navaratnarajah and Indraratna (2017) | Ballast box test | Ballast depth: 300 mm UBM depth: 10 mm Weight 9.2 kg/m ² C _{static} : 0.2 N/mm ³ C _{dyn} : 0.46-0.59 N/mm ³ Load frequency: 10,15,20,25 Hz Load amplitude: 250, 350 kN | <ul style="list-style-type: none"> • 10-20% reduction in vertical strain • 5-10% reduction in lateral strain • 35-45% reduction in degradation (BBI) • 20% reduction in stress at the ballast/sleeper interface • Efficient performance of UBMs on a stiff subgrade rather than the soft one |
| Nimbalkar et al. (2012) | Impact loading test | Ballast depth: 300 mm UBM depth: 30 mm Weight 9.2 kg/m ² C _{static} : 0.2 N/mm ³ C _{dyn} : 0.46-0.59 N/mm ³ (soft and hard UBM) Dynamic stress: 400–600 kPa Impact blows: 10 times | <ul style="list-style-type: none"> • 19% reduction of BBI on stiff subgrade • 24% reduction of BBI on weak subgrade |
| Lima et al. (2017) | Ballast Box test | Ballast PSD: AREMA_No. 4A Ballast depth: 300 mm UBM depth: 5, 10 mm Load frequency: 5 Hz Load amplitude: 1.8 – 26 kN | <ul style="list-style-type: none"> • Ignorable changes in ballast breakage under low force magnitude and frequency |

| | | | |
|--------------------------|---------------------|--|--|
| Diego et al. (2017) | Fatigue test | <p>Using ballast plate: $C_{static} \sim 0.0139 \text{ N/mm}^3$ $C_{static,h} > 0.0050 \text{ N/mm}^3$ C_{dyn} measurement: 1000 initial loading cycles Cyclic load amplitude: 1.8–9 kN Cyclic load frequency: a) 1, 5, 10, 20 Hz at room temperature b) 10 Hz at -20, -10, 0, 30 °C</p> | <ul style="list-style-type: none"> • 135% increase in C_{dyn} when load frequency raised from 1 to 20 Hz • 60% drop in C_{dyn} when temperature raised from -20 to 30 °C • 13 mm settlement after 1st $5 \cdot 10^5$ cycles • 10 mm settlement after 2nd $5 \cdot 10^5$ cycles • 26.2% increase in C_{static} for frost damage test |
| Indraratna et al. (2021) | Impact loading test | <p>Ballast depth 350 mm UBM depth: 10 mm UBM weight: 10.5 kg/m² C_{static}: 0.142 kg/m³ C_{dyn}: 0.107 kg/m³ Load: 5.81 kN Load speed: 10 m/s</p> | <ul style="list-style-type: none"> • 7 – 15% decrease in ballast vertical and lateral deformation • 28% and 10-17% reduction in ballast breakage (BBI) for hard and soft subgrade, respectively |
| Esmaili et al. (2020) | Field test | <p>Granular WTR pillow between ballast and bridge Ballast depth: 200 mm Rubber size: 20 – 50 mm Rubber pillow depth: 0, 100, 200, and 300 mm Train load: 75, 100, 125 kN Train speed: 40, 60, 80, 100 km/h</p> | <ul style="list-style-type: none"> • Using a 300 mm rubber pillow led to a) 52%, 66%, 73, and 50% decrease in bridge deck acceleration, b) 56%, 60%, 43%, and 40% increase in rail acceleration, c) 13%, 11%, 7% and 25% reduction in bridge vertical displacement, when train speed was 40, 60, 80 and 100 km/h, respectively. |

356 2.4 Implementation of investigated WTR products in practical applications

357 Numerous projects focus on the application of WTR in railway tracks, particularly for the
358 mitigation of noise and vibration; however, few projects are available for the application of WTR
359 in ballast deformation and stress reduction, which can be attributed to the uncertainty of the long-
360 term performance of WTR-made products. The following are examples of projects that use WTR
361 products in ballasted railway superstructures:

- 362 • Application of rail dampers in Germany and France to reduce rail noise and vibration
363 (Lakušić and Ahac, 2012).
- 364 • Installing rubber level crossing in Germany manufactured by (STRAIL, 2022).

- 365 • Application of USPs in the Tehran–Mashhad railway in Iran to reduce train-induced
366 vibrations that adversely affect the track infrastructure and its surroundings, as reported by
367 Zakeri et al. (2016).
- 368 • Application of rubber-coated sleeper (GREENRAIL) in the line Reggio Emilia – Sassuolo,
369 Italy (Emilia, 2018) to reduce ballast degradation and vibration.
- 370 • Application of tire-infilled granular waste materials in Chullora Railway (Sydney, 2022),
371 to reduce vertical stress on the subgrade and improve lateral track resistance.

372 Notably, the use of granular WTR mixed with ballast has not been widely implemented in practice
373 because of the uncertainty associated with its behaviour within discrete ballast particles. The
374 complex interaction between the WTR and ballast particles can affect the mechanical properties
375 of the mixture, and there is limited knowledge of its long-term performance and durability under
376 various environmental conditions. Therefore, further research is required to address the challenges
377 and uncertainties associated with the implementation of WTR ballast mixtures in railway
378 trackbeds.

379 **3 Numerical simulation rubber elements**

380 Numerical modelling of rubber-like materials allows for the analysis of their behaviour under
381 diverse circumstances. This encompasses the simulation of deformation and stress–strain
382 behaviour, the prediction of thermal and electrical properties, and their interaction with other
383 components in the track system. The discrete element method (DEM) and finite element method
384 (FEM) are two useful techniques for modelling rubber inclusions in ballasted tracks. Researchers
385 have employed elastic linear contact models to provide a simplified model of the interaction
386 between rubber elements and rigid railway components. Nonlinear/hyperelastic contacts have also

387 been employed for specific scenarios. In the following sections, we describe the techniques applied
388 and the potential challenges for future investigations.

389 **3.1 Finite element method**

390 Several continuum methods have been developed to model the mechanical behaviour of materials,
391 including the boundary element method (BEM), finite element method (FEM), and finite
392 difference method (FDM). For modelling layered WTRs (RPs, USPs, and UBM), FEM is the
393 most commonly used method (Ferreira and López-Pita, 2013). In general, unlike the DEM, the
394 FEM has difficulty replicating multifracture states in solids (Oñate et al., 2018). However, the
395 FEM allows the discretisation of the geometry (rubber products) into small elements that can be
396 connected to form a mesh. The behaviour of each element can be approximated using the
397 constitutive model and equations of motion, and the overall behaviour of the material can be
398 obtained by combining the responses of all the elements. This allows for the accurate prediction
399 of the deformation and stress distribution within a material, which is desirable for simulating large
400 deformable rubber-like materials (Latham et al., 2020).

401 **3.1.1 Constitutive models of rubber particles**

402 In many studies, a linear elastic model has been used for the simulation of soft-rigid contacts,
403 which is given by:

$$\sigma = E\varepsilon = E\frac{\delta}{L} \quad (2)$$

404 Owing to the nonlinear behaviour of rubber, a hyperelastic model may be suitable for modelling
405 the interaction between WTRs and rigid railway components. Hyperelasticity is a constitutive
406 model used to describe the nonlinear behaviour of materials resembling rubber that undergo
407 significant elastic deformation. A hyperelastic material is often characterised by a strain energy

408 density function in the finite element method (FEM), which connects the deformation of the
409 material to its energy. The strain energy density function is generally described in terms of the
410 invariants of the deformation tensor, such as stretches or primary strains. Several methods have
411 been developed for the hyperelastic modelling of materials, such as the Arruda–Boyce, Marlow,
412 Mooney–Rivlin, Neo-Hookean, Ogden, and polynomial methods (Ali et al., 2010). Marckmann
413 and Verron (2005) categorised 19 hyperelastic models in terms of their validity domain for traction
414 (T), pure shear (PS), equibiaxial extension (EQB), and biaxial extension (BE) for Treloar data
415 considering the following assumptions: I) If the accuracy is good, the parameters are retained. II)
416 If the accuracy is poor, the validity domain is modified as follows: a) If the model cannot reproduce
417 the strain hardening at large strains, the domain of validity is reduced for the uniaxial extension
418 mode (λ_{\max}); b) otherwise, other deformation modes are eliminated from the identification
419 procedure. The domain of validity (λ_{\max}) for the various modes of deformation is observed in the
420 response curves. Depending on the deformation domain evaluated, the neo-Hookean, Mooney, and
421 Ogden models were proposed for small, moderate, and large strains, respectively. The constitutive
422 behaviour of a hyperelastic material is based on the total stress–total strain relationship, where the
423 strain energy density is only a function of the deformation gradient (F), expressed in the principal
424 directions of the stretch. The formulation for the hyperelastic modelling of rubber materials can be
425 found in (Farooq et al., 2021).

426 **3.1.2 FEM-based studies on ballasted railway problems**

427 The FEM has been widely used for modelling layered WTR-reinforced tracks, including RPs,
428 USPs, UBMs, and rail dampers. The displacement, stiffness, and vibration (acceleration) of track
429 components under static, cyclic, or train loading were evaluated using FEM (Indraratna et al.,
430 2021). For instance, Shih et al. (2019) used the FEM to simulate the static response of a railway

431 track reinforced by USPs. The results showed that the USP slightly increased the track settlement
 432 owing to the lower confining pressure in the ballast layer. In addition, Sadeghi et al. (2020)
 433 conducted nonlinear modelling of rail fastening, including the bilinear stiffness and damping
 434 coefficient (C). The effects of the RP stiffness, load frequency, and preload magnitude (as the
 435 principal influencing parameters) on the mechanical behaviour of fastening systems were explored
 436 through parametric analyses of fastening systems. Given the FEM-based analyses in Table 9, the
 437 FEM is suitable for investigating the impact of padded rubber on railway infrastructure
 438 performance, particularly track vibration, stiffness, and plane stress distribution.

439 Table 9 FEM-based studies on rubber-used railway superstructure

| Author | Loading type | WTR type | WTR Contact model | Outputs | View |
|-----------------------|---|----------|--------------------------------|---|------|
| Chen et al. (2013) | Fastening system vertical/lateral loading | RP | Linear elastic | <ul style="list-style-type: none"> Tensile and compressive stress of superstructure components | |
| Othman et al. (2022) | Fastening system vertical loading | RP | Hyperelastic (Neo-Hookean) | <ul style="list-style-type: none"> RP stiffness | |
| Sadeghi et al. (2020) | Fastening cyclic loading test | RP | Nonlinear (mathematical model) | <ul style="list-style-type: none"> Rubber stiffness | |

| | | | | | |
|-------------------------------|------------------------------------|-----------------------|---|---|--|
| Kuchak et al. (2021) | Rail shaking | Rail damper | Linear elastic | <ul style="list-style-type: none"> • Decay rate • Rail noise • Rail vibration | |
| Insa et al. (2014) | Train moving load | RP USP | Linear elastic | <ul style="list-style-type: none"> • Track stiffness • Track vibration | |
| Alves Ribeiro et al. (2015) | Passenger tilting train load | USP | Nonlinear | <ul style="list-style-type: none"> • Track vibration • Track settlement | |
| Diego et al. (2017) | Vertical static and cyclic loading | UBM | Non-linear-Hyperelastic (Mooney-Rivlin) | <ul style="list-style-type: none"> • Static/Dynamic bedding modulus | |
| Esmaeili and Siahkouhi (2019) | Train moving load | Impact absorber (UBM) | Linear elastic | <ul style="list-style-type: none"> • Bridge deflection • Bridge vibration | |
| Farooq et al. (2021) | Train loading | USP UBM | Hyper elastic | <ul style="list-style-type: none"> • Track vibration • Track settlement • Vertical stress • Horizontal stress | |

440 3.2 Discrete element method

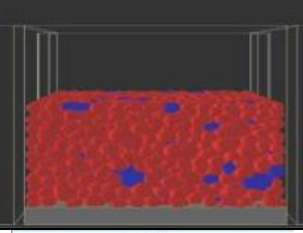
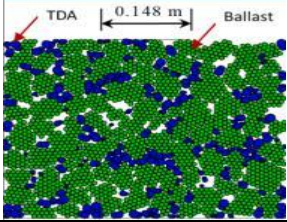
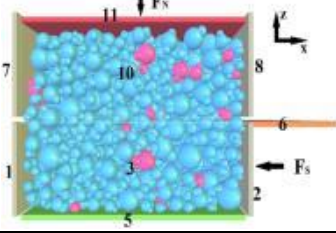
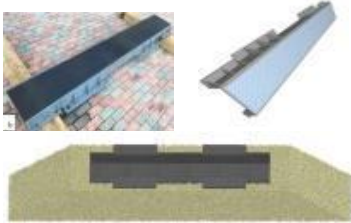

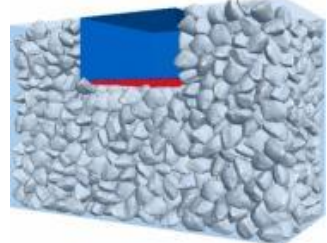
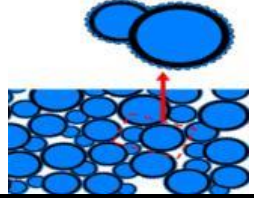
441 The DEM has been widely used to simulate granular materials, considering the discrete and
442 continuum characteristics of particles (Jing and Stephansson, 2007). Although numerous
443 investigations have been performed on sand–rubber contact using numerical methods (particularly

444 DEM), there are few studies on the numerical modelling of rubber elements in ballasted railway
 445 tracks. The DEM may be useful for simulating granular WTR-reinforced railways. According to
 446 previous studies, the linear spring–dashpot and Hertz–Mindlin models have been adopted for the
 447 simulation of contacts between rigid elements. Different methods have been proposed for
 448 modelling deformable materials, including bonded pebbles, elastic clumps, deformable spheres,
 449 and flexible polyhedra. Owing to the irregular shape of granular WTR, bonded pebbles, elastic
 450 clumps, and flexible polyhedrons are suitable alternatives for the accurate analysis of soft-rigid
 451 contacts in railway superstructures.

452 Given the nonhomogeneous behaviour of granular WTR, the DEM might be a better alternative to
 453 provide a particle-scale analysis of WTR-reinforced railway components. In this regard, the DEM
 454 has been mainly used to simulate granular WTR-reinforced ballast (e.g., rubber-coated ballast and
 455 granular WTR–ballast mixture). Interparticle contact forces significantly govern the behaviour of
 456 granular materials. While the FEM uses approximations to model the contact forces between
 457 particles, the DEM explicitly models particle–particle contact mechanics. Modelling the behaviour
 458 of granular WTR requires accurate modelling of the contact mechanics, and the DEM enables a
 459 more accurate depiction of these forces. Moreover, the DEM can be employed to model the
 460 USP/UBM as a bonded ball layer to evaluate its impact on the ballast force chain, ballast vibration,
 461 degradation, and displacement. Table 10 presents the analyses of the WTR-reinforced ballast
 462 railway components using the DEM.

463 Table 10 DEM-based studies on rubber-used railway superstructure

| Author | Loading type | WTR type | WTR Contact model | Outputs | View |
|--------|--------------|----------|-------------------|---------|------|
|--------|--------------|----------|-------------------|---------|------|

| | | | | | |
|------------------------|--|-----------------------------|----------------|--|---|
| Wu et al. (2021) | Impact loading | Crumb | Hertz-Mindlin | <ul style="list-style-type: none"> The vibration of ballast mixed with granular WTRs |  |
| Guo et al. (2022) | Train loading | Crumb | Linear elastic | <ul style="list-style-type: none"> Wheel/rail contact force Rail displacement Ballast stress-strain |  |
| Gong et al. (2019) | Direct shear test | Crumb | Linear elastic | <ul style="list-style-type: none"> Ballast shear strength Coordination number Ballast breakage |  |
| Wang et al. (2022) | Sleeper lateral resistance | USP | Hertz-Mindlin | <ul style="list-style-type: none"> Sleeper lateral resistance Ballast force chain |   |
| Li and McDowell (2018) | Cyclic loading | USP UBM | Linear elastic | <ul style="list-style-type: none"> Ballast stress-strain Ballast settlement Ballast breakage Coordination number |  |
| Guo et al. (2020a) | -Direct shear force -Vertical Cyclic loading | Granular WTR-coated ballast | Linear elastic | <ul style="list-style-type: none"> Track settlement Track vibration Ballast shear strength Ballast force chain |  |

464 **4 Future research directions**

465 There are specific gaps in the literature regarding each WTR element, as listed in Table 11. For
466 instance, although several studies have been conducted on the use of WTR in the ballast layer,
467 there is limited research on the performance of WTR in rail and sleeper components. Additionally,
468 the effects of environmental factors such as temperature and moisture on the performance of WTR
469 products have not been fully explored. Given the research gaps listed in Table 11, the use of WTR
470 in railway infrastructures poses several challenges that must be addressed to ensure optimal
471 performance.

472 I. *General challenge:* WTR is a temperature-dependent material; therefore, the impact of
473 temperature variation should be considered for the numerical modelling of WTR inclusions
474 in railway infrastructure, particularly when WTR is directly exposed to sunlight (e.g.,
475 granular WTR mixed with ballast and USP).

476 II. *The challenge of granular WTR mixed with ballast:* Heavy rain significantly impacts
477 railway track operation by disturbing the ballast drainage system. In this case, the ballast
478 permeability is governed by the selection of a suitable rubber particle size, content, and
479 shape, which is problematic because these parameters influence the permeability of the
480 ballast–WTR mixture. This can be assessed through experiments and numerical methods.

481 III. *The challenge of rubberised concrete sleepers:* Although many types of research have been
482 conducted on rubberised concrete samples, little is known about the suitable size and
483 percentage of WTR mixed in a concrete sleeper with respect to the standards for railway
484 sleepers. This problem can be evaluated using the FEM–DEM, considering concrete as a
485 continuum and aggregates as embedded discrete elements.

486 IV. *The challenge of studies on WTR-reinforced rail:* As previously mentioned, rail dampers
 487 are used to reduce induced-train noise; however, it is essential to determine the optimum
 488 interval for installing rail dampers along the rails. In addition, the manufacture and analysis
 489 of WTR-made sound protection walls fastened to the rail foot, which requires the design
 490 of their size and location along the trackside, will be of great interest.

491 Table 11 Relationship between WTR products and influential parameters

| Parameters | Railway components | | | | | | | | | | |
|---|--------------------|-------------|----------------------|---------|----|-----------------------|----------|---------|---------|--------------------------|--------------|
| | Rail | | | Sleeper | | | | Ballast | | | |
| | RP | Rail damper | Level crossing panel | USP | RC | Rubber-coated sleeper | FRP tube | UBM | GRIDMAT | Granular WTR-ballast mix | Rubber tyres |
| Rail noise | ✓ | ✓ | ✓ | | | | | | | | |
| Rail vibration | ✓ | ✓ | | ✓ | | | | | | | |
| Rail corrugation | ✓ | ✓ | | ✓ | | | | | | | |
| Electrical resistance | | | ✓ | | ✓ | | | | | | |
| Sleeper fatigue strength | | | | | ✓ | | | | | | |
| Sleeper impact resistance | | | | | ✓ | | | | | | |
| Sleeper vibration | | | | | ✓ | | | | | | |
| Sleeper damage | | | | | ✓ | | | | | | |
| Compressive/ flexural/tensile strength | | | | | ✓ | | ✓ | | | | |
| Chemical properties | | | | | ✓ | | | | | | |
| Ballast settlement | | | | ✓ | | ✓ | | ✓ | ✓ | ✓ | ✓ |
| Ballast stress distribution | | | | ✓ | | ✓ | | ✓ | ✓ | ✓ | ✓ |
| Ballast breakage | | | | ✓ | | ✓ | | ✓ | ✓ | ✓ | |
| Ballast lateral resistance | | | | ✓ | | | | ✓ | | | ✓ |
| Track stiffness | ✓ | ✓ | | ✓ | | ✓ | | ✓ | ✓ | ✓ | |
| Ballast damping | ✓ | | | ✓ | | ✓ | | ✓ | ✓ | ✓ | |
| Ballast acceleration | ✓ | | | ✓ | | | | ✓ | ✓ | ✓ | |

492 **5 Conclusion**

493 In this review, we explored the potential benefits of utilising WTR in the ballasted superstructure
494 of railway tracks, including the rail, sleeper, and ballast layers. Rubber can be used in the form of
495 pads or granules of varying sizes depending on its specific application. This study provides a
496 comprehensive evaluation of the performance of WTR-reinforced ballasted tracks in terms of
497 vibration, noise, stiffness, settlement, breakage, damping, shear strength, and lateral resistance.
498 The results from experimental studies have highlighted the effectiveness of rubber-reinforced
499 railways in reducing noise and vibration, altering track stiffness, and improving overall
500 performance. Moreover, the development of numerical modelling using the DEM or FEM is
501 discussed to analyse the performance of rubber-reinforced railway tracks. Such modelling can aid
502 in optimising the design of railway tracks, leading to improved safety, reduced maintenance costs,
503 and extended service life. Overall, this study indicated that the use of WTR in railway
504 infrastructure has significant potential and warrants further investigation to fully understand their
505 benefits and limitations.

506 **Acknowledgement**

507 We acknowledge the support of the National Science Foundation of China (NSFC) [52027813]
508 for this paper.

509 **ReferencesUncategorized References**

- 510 Akinyele, J.O., Salim, R.W., Kupolati, W.K., 2015. The impact of rubber crumb on the mechanical and
511 chemical properties of concrete. *Engineering Structures and Technologies* 7(4), 197-204.
- 512 Ali, A., Hosseini, M., Sahari, B., 2010. A review of constitutive models for rubber-like materials. *American*
513 *Journal of Engineering and Applied Sciences* 3(1), 232-239.
- 514 Alves Ribeiro, C., Paixão, A., Fortunato, E., Calçada, R., 2015. Under sleeper pads in transition zones at
515 railway underpasses: numerical modelling and experimental validation. *Structure and Infrastructure*
516 *Engineering* 11(11), 1432-1449.
- 517 Arachchige, C.M.K., Indraratna, B., Qi, Y., Vinod, J.S., Rujikiatkamjorn, C., 2022a. Deformation and
518 degradation behaviour of Rubber Intermixed Ballast System under cyclic loading. *Engineering Geology*
519 307, 106786.
- 520 Arachchige, C.M.K., Indraratna, B., Qi, Y., Vinod, J.S., Rujikiatkamjorn, C., 2022b. Geotechnical
521 characteristics of a Rubber Intermixed Ballast System. *Acta Geotechnica* 17(5), 1847-1858.
- 522 ASTM D6270-20, 2020. Standard Practice for Use of Scrap Tires in Civil Engineering Applications, ASTM
523 International, West Conshohocken, PA, . ASTM, <https://www.astm.org/d6270-20.html>, p. 22.
- 524 Batayneh, M.K., Marie, I., Asi, I., 2008. Promoting the use of crumb rubber concrete in developing
525 countries. *Waste Management* 28(11), 2171-2176.
- 526 Bompa, D.V., Elghazouli, A.Y., Xu, B., Stafford, P.J., Ruiz-Teran, A.M., 2017. Experimental assessment and
527 constitutive modelling of rubberised concrete materials. *Construction and Building Materials* 137, 246-
528 260.
- 529 BS_EN16730, 2016. Railway applications — Track —Concrete sleepers and bearerswith under sleeper
530 pads. BSI Standards Limited, UK
- 531 BS_EN17282, 2020. Railway applications. Infrastructure. Under ballast mats. BSI Standards Limited, UK
- 532 CalRecycle, 2001. Tire-Derived Aggregate as Vibration Mitigation.
- 533 Carrascal, I., Casado, J., Diego, S., Polanco, J., Gutiérrez-Solana, F., 2010. Efecto del envejecimiento de
534 placas de asiento de carril inyectadas con TPE en la elasticidad de la vía para Alta Velocidad, 31st Meeting
535 of the Spanish Group of Crack ‘Grupo Español de Fractura.
- 536 Carrascal Vaquero, I.A., 2010. Optimización y análisis de comportamiento de sistemas de sujeción para
537 vías de ferrocarril de alta velocidad española.
- 538 Chen, Z., Shin, M., Andrawes, B., 2013. Finite element modeling of the fastening systems and the concrete
539 sleepers in North America, Proceedings of the 2013 International Heavy Haul Association Conference.
540 New Delhi, India,(February 2013).
- 541 Diego, S., Casado, J., Carrascal, I., Ferreño, D., Cardona, J., Arcos, R., 2017. Numerical and experimental
542 characterization of the mechanical behavior of a new recycled elastomer for vibration isolation in railway
543 applications. *Construction and Building Materials* 134, 18-31.
- 544 Dolci, G., Rigamonti, L., Grosso, M., 2020. Potential for improving the environmental performance of
545 railway sleepers with an outer shell made of recycled materials. *Transportation Research Interdisciplinary*
546 *Perspectives* 6, 100160.

- 547 Egana, J.I., Vinolas, J., Seco, M., 2006. Investigation of the influence of rail pad stiffness on rail corrugation
548 on a transit system. *Wear* 261(2), 216-224.
- 549 Emilia, R., 2018. The first smart railway stretch of new generation presented on the line Reggio Emilia –
550 Sassuolo.
- 551 Esmaeili, M., Aela, P., Hosseini, A., 2017. Experimental assessment of cyclic behavior of sand-fouled ballast
552 mixed with tire derived aggregates. *Soil Dynamics and Earthquake Engineering* 98, 1-11.
- 553 Esmaeili, M., Ataei, S., Siahkouhi, M., 2020. A case study of dynamic behaviour of short span concrete slab
554 bridge reinforced by tire-derived aggregates as sub-ballast. *International Journal of Rail Transportation*
555 8(1), 80-98.
- 556 Esmaeili, M., Farsi, S., Shamohammadi, A., 2022. Effect of rock strength on the degradation of ballast
557 equipped with under sleeper pad. *Construction and Building Materials* 321, 126413.
- 558 Esmaeili, M., Namaei, P., 2022. Effect of mother rock strength on rubber-coated ballast (RCB)
559 deterioration. *Construction and Building Materials* 316, 126106.
- 560 Esmaeili, M., Siahkouhi, M., 2019. Tire-derived aggregate layer performance in railway bridges as a novel
561 impact absorber: Numerical and field study. *Structural Control and Health Monitoring* 26(10), e2444.
- 562 Fakhri, M., Saberi, K, F., 2016. The effect of waste rubber particles and silica fume on the mechanical
563 properties of Roller Compacted Concrete Pavement. *Journal of Cleaner Production* 129, 521-530.
- 564 Farooq, M.A., Nimbalkar, S., Fatahi, B., 2021. Three-dimensional finite element analyses of tyre derived
565 aggregates in ballasted and ballastless tracks. *Computers and Geotechnics* 136, 104220.
- 566 Fathali, M., Esmaeili, M., Moghadas Nejad, F., 2019. Influence of tire-derived aggregates mixed with
567 ballast on ground-borne vibrations. *Journal of Modern Transportation* 27(4), 355-363.
- 568 Fathali, M., Nejad, F.M., Esmaeili, M., 2017. Influence of Tire-Derived Aggregates on the Properties of
569 Railway Ballast Material. *Journal of Materials in Civil Engineering* 0(0), 04016177.
- 570 Feng, L.-Y., Chen, A.-J., Liu, H.-D., 2022. Experimental Study on the Property and Mechanism of the
571 Bonding Between Rubberized Concrete and Normal Concrete. *International Journal of Concrete*
572 *Structures and Materials* 16(1), 1-12.
- 573 Ferdous, W., Manalo, A., AlAjarmeh, O.S., Zhuge, Y., Mohammed, A.A., Bai, Y., Aravinthan, T., Schubel, P.,
574 2021. Bending and Shear Behaviour of Waste Rubber Concrete-Filled FRP Tubes with External Flanges.
575 *Polymers* 13(15), 2500.
- 576 Ferreira, P.A., López-Pita, A., 2013. Numerical Modeling of High-Speed Train/Track System to Assess Track
577 Vibrations and Settlement Prediction. *Journal of Transportation Engineering* 139(3), 330-337.
- 578 Fontserè, V., Pita, A.L., Manzo, N., Ausilio, A., 2016. NEOBALLAST: new high-performance and long-lasting
579 ballast for sustainable railway infrastructures. *Transportation Research Procedia* 14, 1847-1854.
- 580 Giannakos, K., 2010. Influence of rail pad stiffness on track stressing, life-cycle and noise emission,
581 *Proceedings of the 2nd International Conference on Sustainable Construction Materials and Technologies.*
582 *Università Politecnica delle Marche.*
- 583 Gong, H., Song, W., Huang, B., Shu, X., Han, B., Wu, H., Zou, J., 2019. Direct shear properties of railway
584 ballast mixed with tire derived aggregates: Experimental and numerical investigations. *Construction and*
585 *Building Materials* 200, 465-473.

586 Grassie, S., 1989. Resilient railpads: their dynamic behaviour in the laboratory and on track. Proceedings
587 of the Institution of Mechanical Engineers, Part F: Journal of Rail and Rapid Transit 203(1), 25-32.

588 Guo, Y., Ji, Y., Zhou, Q., Markine, V., Jing, G., 2020a. Discrete Element Modelling of Rubber-Protected
589 Ballast Performance Subjected to Direct Shear Test and Cyclic Loading. Sustainability 12(7), 2836.

590 Guo, Y., Markine, V., Qiang, W., Zhang, H., Jing, G., 2019. Effects of crumb rubber size and percentage on
591 degradation reduction of railway ballast. Construction and Building Materials 212, 210-224.

592 Guo, Y., Shi, C., Zhao, C., Markine, V., Jing, G., 2022. Numerical analysis of train-track-subgrade dynamic
593 performance with crumb rubber in ballast layer. Construction and Building Materials 336, 127559.

594 Guo, Y., Wang, J., Markine, V., Jing, G., 2020b. Ballast Mechanical Performance with and without Under
595 Sleeper Pads. KSCE Journal of Civil Engineering 24(11), 3202-3217.

596 Hameed, A.S., Shashikala, A.P., 2016. Suitability of rubber concrete for railway sleepers. Perspectives in
597 Science 8, 32-35.

598 Hans Bendtsen, S.T., 2007. Noise from Railway Crossings, Danish Road Institute Report 152. Road
599 Directorate_Ministry of Transport and Energy, Hedehusene, Denmark.

600 Ho, C.L., Humphrey, D., Hyslip, J.P., Moorhead, W., 2013. Use of Recycled Tire Rubber to Modify Track-
601 Substructure Interaction. Transportation Research Record 2374(1), 119-125.

602 Humphrey, D., 2007. Tire derived aggregate as lightweight fill for embankments and retaining walls,
603 Proceedings International Workshop on Scrap Tire Derived Geomaterials, Yokosuka, Japan. pp. 59-81.

604 Ilias, H., 1999. The influence of railpad stiffness on wheelset/track interaction and corrugation growth.
605 Journal of Sound and Vibration 227(5), 935-948.

606 Indraratna, B., Mehmood, F., Mishra, S., Ngo, T., Rujikiatkamjorn, C., 2022a. The role of recycled rubber
607 inclusions on increased confinement in track substructure. Transportation Geotechnics 36, 100829.

608 Indraratna, B., Qi, Y., Jayasuriya, C., Rujikiatkamjorn, C., Arachchige, C.M.K., 2021. Use of recycled rubber
609 inclusions with granular waste for enhanced track performance. Transportation Engineering 6, 100093.

610 Indraratna, B., Qi, Y., Malisetty, R.S., Navaratnarajah, S.K., Mehmood, F., Tawk, M., 2022b. Recycled
611 materials in railroad substructure: an energy perspective. Railway Engineering Science 30(3), 304-322.

612 Insa, R., Salvador, P., Inarejos, J., Medina, L., 2014. Analysis of the performance of under-sleeper pads in
613 high-speed line transition zones. Proceedings of the Institution of Civil Engineers - Transport 167(2), 63-
614 77.

615 Jing, G., Fu, H., Aela, P., 2018. Lateral displacement of different types of steel sleepers on ballasted track.
616 Construction and Building Materials 186, 1268-1275.

617 Jing, G., Siahkouhi, M., Riley Edwards, J., Dersch, M.S., Hout, N.A., 2021. Smart railway sleepers - a review
618 of recent developments, challenges, and future prospects. Construction and Building Materials 271,
619 121533.

620 Jing, G., yunchang, D., You, R., Siahkouhi, M., 2022. Comparison study of crack propagation in rubberized
621 and conventional prestressed concrete sleepers using digital image correlation. Proceedings of the
622 Institution of Mechanical Engineers, Part F: Journal of Rail and Rapid Transit 236(4), 350-361.

623 Jing, L., Stephansson, O., 2007. Fundamentals of discrete element methods for rock engineering: theory
624 and applications. Elsevier.

625 Johansson, A., Nielsen, J.C.O., Bolmsvik, R., Karlström, A., Lundén, R., 2008. Under sleeper pads—Influence
626 on dynamic train–track interaction. *Wear* 265(9), 1479-1487.

627 Kaewunruen, S., Li, D., Chen, Y., Xiang, Z., 2018. Enhancement of Dynamic Damping in Eco-Friendly Railway
628 Concrete Sleepers Using Waste-Tyre Crumb Rubber. *Materials (Basel)* 11(7).

629 Koohmishi, M., Azarhoosh, A., 2020. Hydraulic conductivity of fresh railway ballast mixed with crumb
630 rubber considering size and percentage of crumb rubber as well as aggregate gradation. *Construction and*
631 *Building Materials* 241, 118133.

632 Koohmishi, M., Azarhoosh, A., 2021. Degradation of crumb rubber modified railway ballast under impact
633 loading considering aggregate gradation and rubber size. *Canadian Geotechnical Journal* 58(3), 398-410.

634 Koohmishi, M., Azarhoosh, A., 2022. Assessment of Performance of Recycled Ballast Aggregate Subjected
635 to Drop-Weight Impact Loading Considering Effect of Crumb Rubber Incorporation. *Journal of Materials*
636 *in Civil Engineering* 34(5), 04022057.

637 Kraśkiewicz, C., Chmielewska, B., Zbiciak, A., Al Sabouni-Zawadzka, A., 2021. Study on Possible Application
638 of Rubber Granulate from the Recycled Tires as an Elastic Cover of Prototype Rail Dampers, with a Focus
639 on Their Operational Durability. *Materials* 14(19), 5711.

640 Kraśkiewicz, C., Zbiciak, A., Al Sabouni-Zawadzka, A., Piotrowski, A., 2022. Resistance to severe
641 environmental conditions of prototypical recycling-based under ballast mats (UBMs) used as vibration
642 isolators in the ballasted track systems. *Construction and Building Materials* 319, 126075.

643 Kraśkiewicz, C., Zbiciak, A., Oleksiewicz, W., Karwowski, W., 2018. Static and dynamic parameters of
644 railway tracks retrofitted with under sleeper pads. *Archives of Civil Engineering* Vol. 64(No 4/II), 187-201.

645 Kraśkiewicz, C., Zbiciak, A., Pełczyński, J., Al Sabouni-Zawadzka, A., 2023. Experimental and numerical
646 testing of prototypical under ballast mats (UBMs) produced from deconstructed tires – The effect of mat
647 thickness. *Construction and Building Materials* 369, 130559.

648 Kuchak, A.J.T., Marinkovic, D., Zehn, M., 2021. Parametric Investigation of a Rail Damper Design Based on
649 a Lab-Scaled Model. *Journal of Vibration Engineering & Technologies* 9(1), 51-60.

650 Lakušić, S., Ahac, M., 2012. Rail traffic noise and vibration mitigation measures in urban areas. *Technical*
651 *Gazette* 19(2), 427-435.

652 Latham, J.-P., Xiang, J., Farsi, A., Joulin, C., Karantzoulis, N., 2020. A class of particulate problems suited to
653 FDEM requiring accurate simulation of shape effects in packed granular structures. *Computational Particle*
654 *Mechanics* 7(5), 975-986.

655 Leykauf, G., Stahl, W., 2004. Untersuchungen und Erfahrungen mit besohlenen Schwellen. *Der*
656 *Eisenbahningenieur (Hamburg)* 55(6), 8-16.

657 Li, H., McDowell, G.R., 2018. Discrete element modelling of under sleeper pads using a box test. *Granular*
658 *Matter* 20(2), 26.

659 Li, W., Huang, Z., Wang, X.C., Wang, J.W., 2014. Review of Crumb Rubber Concrete. *Applied Mechanics*
660 *and Materials* 672-674, 1833-1837.

661 Lima, A.d.O., Dersch, M., Qian, Y., Tutumluer, E., Edwards, J., 2017. Laboratory evaluation of under-ballast
662 mat effectiveness to mitigate differential movement problem in railway transition zones, *Bearing Capacity*
663 *of Roads, Railways and Airfields*. CRC Press, pp. 1969-1975.

- 664 Loy, H., 2008. Under sleeper pads: improving track quality while reducing operational costs. *European*
665 *Railway Review* 4, 46-51.
- 666 Maes, J., Sol, H., Guillaume, P., 2006. Measurements of the dynamic railpad properties. *Journal of Sound*
667 *and Vibration* 293(3-5), 557-565.
- 668 Marckmann, G., Verron, E., 2005. Efficiency of hyperelastic models for rubber-like materials,
669 CONSTITUTIVE MODELS FOR RUBBER-PROCEEDINGS-. Balkema, p. 375.
- 670 Marschnig, S., Ehrhart, U., Offenbacher, S., 2022. Long-Term Behaviour of Padded Concrete Sleepers on
671 Reduced Ballast Bed Thickness. *Infrastructures* 7(10), 132.
- 672 Mayuranga, H.G.S., Navaratnarajah, S.K., Bandara, C.S., Jayasinghe, J.A.S.C., 2023. Elastic inclusions in
673 ballasted tracks – a review and recommendations. *International Journal of Rail Transportation*, 1-28.
- 674 Mayuranga, S., Navaratnarajah, S., Bandara, C., Jayasinghe, J.A.S.C., 2020. A STATE OF THE ART REVIEW
675 OF THE INFLUENCE OF RUBBER INCLUSIONS IN RAILWAY TRACKS, 10th International Conference on
676 Structural Engineering and Construction Management (ICSECM).
- 677 Meesit, R., Kaewunruen, S., 2017. Vibration Characteristics of Micro-Engineered Crumb Rubber Concrete
678 for Railway Sleeper Applications. *Journal of Advanced Concrete Technology* 15(2), 55-66.
- 679 Mohajerani, A., Burnett, L., Smith, J.V., Markovski, S., Rodwell, G., Rahman, M.T., Kurmus, H., Mirzababaei,
680 M., Arulrajah, A., Horpibulsuk, S., 2020. Recycling waste rubber tyres in construction materials and
681 associated environmental considerations: A review. *Resources, Conservation and Recycling* 155, 104679.
- 682 Mohammed, B.S., Adamu, M., Shafiq, N., 2017. A review on the effect of crumb rubber on the properties
683 of rubbercrete. *Int. J. Civ. Eng. Technol* 8(9), 599-615.
- 684 Müller, R., Brechbühl, Y., 2013. Measurement report about a new under sleeper test track in a curve. Rivas
685 project Deliverable 3.
- 686 Najim, K.B., Hall, M.R., 2010. A review of the fresh/hardened properties and applications for plain- (PRC)
687 and self-compacting rubberised concrete (SCRC). *Construction and Building Materials* 24(11), 2043-2051.
- 688 Navaratnarajah, S.K., Indraratna, B., 2017. Use of Rubber Mats to Improve the Deformation and
689 Degradation Behavior of Rail Ballast under Cyclic Loading. *Journal of Geotechnical and Geoenvironmental*
690 *Engineering* 143(6), 04017015.
- 691 Navaratnarajah, S.K., Indraratna, B., Ngo, N.T., 2018. Influence of Under Sleeper Pads on Ballast Behavior
692 Under Cyclic Loading: Experimental and Numerical Studies. *Journal of Geotechnical and*
693 *Geoenvironmental Engineering* 144(9), 04018068.
- 694 Ngamkhanong, C., Kaewunruen, S., 2020. Effects of under sleeper pads on dynamic responses of railway
695 prestressed concrete sleepers subjected to high intensity impact loads. *Engineering Structures* 214,
696 110604.
- 697 Nimbalkar, S., Indraratna, B., Dash, S.K., Christie, D., 2012. Improved performance of railway ballast under
698 impact loads using shock mats. *Journal of Geotechnical and Geoenvironmental Engineering* 138(3), 281-
699 294.
- 700 Noaman, A.T., Abu Bakar, B.H., Akil, H.M., 2016. Experimental investigation on compression toughness of
701 rubberized steel fibre concrete. *Construction and Building Materials* 115, 163-170.
- 702 Oikonomou, N., Mavridou, S., 2009. The use of waste tyre rubber in civil engineering works, *Sustainability*
703 *of construction materials*. Elsevier, pp. 213-238.

704 Omodaka, A., Kumakura, T., Konishi, T., 2017. Maintenance Reduction by the Development of Resilient
705 Sleepers for Ballasted Track with Optimal Under-sleeper Pads. *Procedia CIRP* 59, 53-56.

706 Oñate, E., Zárate, F., Celigueta, M.A., González, J.M., Miquel, J., Carbonell, J.M., Arrufat, F., Latorre, S.,
707 Santasusana, M., 2018. Advances in the DEM and coupled DEM and FEM techniques in non linear solid
708 mechanics, *Advances in computational plasticity*. Springer, pp. 309-335.

709 Othman, M.I.H., Abdul Wahab, A.M., Hadi, M.S., Mohamad Noor, N., 2022. Assessing the nonlinear static
710 stiffness of rail pad using finite element method. *Journal of Vibroengineering* 24(5), 921-935.

711 PANDROL, 2021. In accordance with ISO 14025 and EN 15804:2012+A1:2013 for: Under Sleeper Pad, type
712 USP-I-07d-MFF.

713 Qi, W., Aela, P., Jing, G., Tong, Y., Rad, M.M., 2022. Optimization of the Angled Guide Plate for the Vossloh
714 W14-PK Fastener. *Acta Polytechnica Hungarica* 19(6).

715 RosehillRail, 2022. Rail Crossing Solutions, in: Rail, R. (Ed.). <https://rosehillrail.com/>.

716 Sadeghi, J., Seyedkazemi, M., Khajehdezfuly, A., 2020. Nonlinear simulation of vertical behavior of railway
717 fastening system. *Engineering Structures* 209, 110340.

718 Schneider, P., Bolmsvik, R., Nielsen, J.C.O., 2011. In situ performance of a ballasted railway track with
719 under sleeper pads. *Proceedings of the Institution of Mechanical Engineers, Part F: Journal of Rail and
720 Rapid Transit* 225(3), 299-309.

721 Shih, J.-Y., Grossoni, I., Bezin, Y., 2019. Settlement analysis using a generic ballasted track simulation
722 package. *Transportation Geotechnics*, 100249.

723 Siahkouhi, M., Li, C., Astaraki, F., Rad, M.M., Fischer, S., Jing, G., 2022. Comparative Study of the
724 Mechanical Behavior of Concrete Railway Sleeper Mix Design, using Waste Rubber and Glass Materials.
725 *Acta Polytechnica Hungarica* 19(6).

726 Siddika, A., Mamun, M.A.A., Alyousef, R., Amran, Y.H.M., Aslani, F., Alabduljabbar, H., 2019. Properties
727 and utilizations of waste tire rubber in concrete: A review. *Construction and Building Materials* 224, 711-
728 731.

729 Siddiqui, A.R., Indraratna, B., Ngo, T., Rujikiatkamjorn, C., 2023. Laboratory assessment of rubber grid-
730 reinforced ballast under impact testing. *Géotechnique Letters* 13(2), 1-11.

731 Sol-Sánchez, M., Mattinzioli, T., Castillo-Mingorance, J.M., Moreno-Navarro, F., Rubio-Gámez, M.C., 2022.
732 GRIDMAT—A Sustainable Material Combining Mat and Geogrid Concept for Ballasted Railways.
733 *Sustainability* 14(18), 11186.

734 Sol-Sánchez, M., Moreno-Navarro, F., Martínez-Montes, G., Rubio-Gámez, M.C., 2017. An alternative
735 sustainable railway maintenance technique based on the use of rubber particles. *Journal of Cleaner
736 Production* 142, 3850-3858.

737 Sol-Sánchez, M., Moreno-Navarro, F., Rubio-Gámez, M.C., 2014a. The use of deconstructed tire rail pads
738 in railroad tracks: Impact of pad thickness. *Materials & Design* 58, 198-203.

739 Sol-Sánchez, M., Moreno-Navarro, F., Rubio-Gámez, M.C., 2014b. Viability analysis of deconstructed tires
740 as material for rail pads in high-speed railways. *Materials & Design* 64, 407-414.

741 Sol-Sánchez, M., Moreno-Navarro, F., Rubio-Gámez, M.C., 2015. The use of elastic elements in railway
742 tracks: A state of the art review. *Construction and Building Materials* 75, 293-305.

743 Sol-Sánchez, M., Moreno-Navarro, F., Tauste-Martínez, R., Saiz, L., Rubio-Gámez, M.C., 2020. Recycling
744 Tire-Derived Aggregate as elastic particles under railway sleepers: Impact on track lateral resistance and
745 durability. *Journal of Cleaner Production* 277, 123322.

746 Sol-Sánchez, M., Thom, N.H., Moreno-Navarro, F., Rubio-Gámez, M.C., Airey, G.D., 2015. A study into the
747 use of crumb rubber in railway ballast. *Construction and Building Materials* 75, 19-24.

748 Song, W., Huang, B., Shu, X., Wu, H., Gong, H., Han, B., Zou, J., 2019. Improving Damping Properties of
749 Railway Ballast by Addition of Tire-Derived Aggregate. *Transportation Research Record* 2673(5), 299-307.

750 Stahl, W., 2005. IMPROVEMENT OF BALLASTED TRACKS USING SLEEPER PADS: INVESTIGATIONS AND
751 EXPERIENCES IN GERMANY, Proceedings of the international conferences on the bearing capacity of
752 roads, railways and airfields.

753 STRAIL, 2022. The Number 1_Level Crossing, in: Co., K.S.G. (Ed.). <https://www.strail.de>.

754 Sydney, U.o.T., 2022. Rubber railway: disrupting a 200-year-old sector.

755 Teixeira, P.F., 2004. Contribución a la reducción de los costes de mantenimiento de vías de alta velocidad
756 mediante la optimización de su rigidez vertical. Universitat Politècnica de Catalunya.

757 Thompson, D., Jones, C., 2006. Noise and vibration from railway vehicles, *Handbook of Railway Vehicle*
758 *Dynamics*. pp. 279-326.

759 Toward, M., Thompson, D., 2012. Laboratory methods for testing the performance of acoustic rail
760 dampers, *Acoustics* 2012.

761 USTMA, 2019. Distribution of scrap tire disposition in the U.S. in 2017 The US Tire Manufacturers
762 Association, Statista. Retrieved January 13, 2023

763 Wang, M., Han, X., Jing, G., Wang, H., 2022. Experimental and numerical analysis on mechanical behaviour
764 of steel turnout sleeper. *Construction and Building Materials* 329, 127133.

765 Werkstoffe, G., 2006. Ballast mats. Characteristics of solutions in service. Paris, UIC.

766 Wu, H., Zhu, L., Song, W., Xu, Z., Xu, F., Gong, H., 2021. Impact performance of ballast by incorporating
767 waste tire-derived aggregates. *Construction and Building Materials* 288, 122992.

768 Xu, C., Chi, M.-R., Dai, L., Guo, Z., 2020. Calculation of Nonlinear Stiffness of Rubber Pad under Different
769 Temperatures and Prepressures. *Shock and Vibration* 2020, 8140782.

770 Zakeri, J.-A., Esmaili, M., Heydari-Noghabi, H., 2016. A field investigation into the effect of under sleeper
771 pads on the reduction of railway-induced ground-borne vibrations. *Proceedings of the Institution of*
772 *Mechanical Engineers, Part F: Journal of Rail and Rapid Transit* 230(3), 999-1005.

773 Zeng, Z., Ahmed Shuaibu, A., Liu, F., Ye, M., Wang, W., 2020. Experimental study on the vibration reduction
774 characteristics of the ballasted track with rubber composite sleepers. *Construction and Building Materials*
775 262, 120766.

776 Zhang, F., Chang, J., Feng, H., 2022. Laboratory study on degradation of ballast mixed with crumb rubber
777 under impact loads. *International Journal of Rail Transportation*, 1-23.

778 Zvolenský, P., Grencik, J., Pultznerová, A., Kašiar, L., 2017. Research of noise emission sources in railway
779 transport and effective ways of their reduction. *MATEC Web of Conferences* 107, 00073.

780